Genetička struktura ugroženog crvenog koralja Corallium rubrum (Linnaeus, 1758) analizirana pomoću mikrosatelitnih lokusa

Stipoljev, Sunčica

Master's thesis / Diplomski rad

2018

Degree Grantor / Ustanova koja je dodijelila akademski / stručni stupanj: **University of Zagreb, Faculty of Science / Sveučilište u Zagrebu, Prirodoslovno-matematički fakultet**

Permanent link / Trajna poveznica: https://urn.nsk.hr/urn:nbn:hr:217:965364

University of Zagreb

Faculty of Science

Department of Biology

Sunčica Stipoljev

Fine-scale genetic structure of the threatened red coral, *Corallium rubrum* (Linnaeus, 1758) inferred from microsatellite markers

Graduation thesis

Zagreb, 2018

This thesis had been conducted at the Institut de Ciències del Mar - Consejo superior de Investigaciones Científicas (CSIC) in Barcelona, Spain, under the supervision of Dr. Jean-Baptiste Ledoux, co-supervision of Dr. Ana Galov, Assoc. Prof. and assistant supervision of Dr. Silvija Kipson. The thesis was submitted for evaluation to the Division of Biology, Faculty of Science, University of Zagreb to acquire the academic title of Master of Ecology and Nature Preservation.

ACKNOWLEDGMENTS

I thank to Dr. Jean-Baptiste Ledoux for mentorship, immense help and patience, and for correcting manuscript of this thesis.

I thank to Dr. Joaquim Garrabou for accepting me as an internship student in his research group and for advices during analysis of samples.

I would like to especially thank Paula López-Sendino MSc. for teaching me laboratory work and for always being there for me when needed.

Many Thanks to Dr. Silvija Kipson and to my professors Ana Galov and Tatjana Bakran-Petricioli for recommending me for this internship and for all their help and support.

BASIC DOCUMENTATION CARD

University of Zagreb
Faculty of Science
Department of Biology

Graduation Thesis

Fine-scale genetic structure of the threatened red coral, *Corallium rubrum* (Linnaeus, 1758) inferred from microsatellite markers

Sunčica Stipoljev

Rooseveltov trg 6, 10000 Zagreb, Croatia

The precious Mediterranean red coral, *Corallium rubrum*, is ecosystem engineer with essential role in structuring and functioning of coralligenous outcrops, which are among the richest but also the most threatened Mediterranean habitats. The main threats to the red coral are intensive historical fishing for its use in jewellery and climate-induced mass mortality events. The high longevity and slow population dynamics of *C. rubrum* make this species exceptionally vulnerable when faced with sources of strong disturbances. In this sense, the knowledge of population dynamics is central for management and conservation purposes. The main objectives of this study were, combining population genetics, spatial distribution analyses and demography, to characterize the pattern of fine-spatial scale genetic and kinship structure among *C. rubrum* colonies over an area of two square meters from a population situated in the marine protected area in the Mediterranean Sea (Scandola, Corsica). Based on these patterns, underlying microevolutionary processes acting in the study population were inferred with particular emphasize on dispersal. Our results demonstrated significant spatial genetic structure (SGS) and individual spatial aggregation within sampled population. Based on this SGS, the mean dispersal within population was estimated to range between 53 and 76 cm, confirming restricted dispersal abilities of this species. Kinship analysis on these samples showed a complex level of half-sib relationships, confirming multiple mating between genetically related colonies suggesting the occurrence of biparental inbreeding. Our results expand previous findings, implying that *C. rubrum* populations are closed and that local processes has a central role in their biology, which has important implications for the conservation of red coral.

(51 pages, 12 figures, 5 tables, 94 references, original in: English)

Thesis deposited in the Central Biological Library

Key words: *Corallium rubrum*, dispersal, genetic drift, kinship structure, spatial genetic structure

Supervisor: Dr. Jean-Baptiste Ledoux

Co-supervisor: Dr. Ana Galov, Assoc. Prof.

Assistant Supervisor: Dr. Silvija Kipson

Reviewers: Dr. Ana Galov, Assoc. Prof.

Dr. Tatjana Bakran-Petricioli, Assoc. Prof.

Dr. Petra Korać, Assoc. Prof.

Thesis accepted: 04.05.2018.

TEMELJNA DOKUMENTACIJSKA KARTICA

Sveučilište u Zagrebu
Prirodoslovno-matematički fakultet
Biološki odsjek **Diplomski rad**

Genetička struktura ugroženog crvenog koralja *Corallium rubrum* (Linnaeus, 1758) analizirana pomoću mikrosatelitnih lokusa

Sunčica Stipoljev

Rooseveltov trg 6, 10000 Zagreb, Hrvatska

Dragocjeni mediteranski crveni koralj, *Corallium rubrum*, je inženjer ekosustava sa esencijalnom ulogom u strukturiranju i funkcioniranju koraligenskih staništa, koja su među najbogatijim, ali također i najugroženijim staništima Mediterana. Glavne prijetnje crvenom koralju su intenzivno povijesno izlovljavanje zbog uporabe u izradi nakita i masovna ugibanja uzrokovana klimatskim promjenama. Dugovječnost i usporena populacijska dinamika čine *C. rubrum* iznimno osjetljivim kada se suočava s izvorima jakih poremećaja. U tom smislu, poznavanje populacijske dinamike je od velike važnosti za gospodarenje i konzervaciju. Glavni ciljevi ovog rada bili su, kombinacijom populacijske genetike, analize prostorne raspodjele i demografije, karakterizirati obrazac genetičke i srodstvene strukture kolonija *C. rubrum* na površini od dva metra kvadratna iz populacije smještene u morskom zaštićenom područje u Sredozemnom moru (Scandola, Korzika). Na temelju tih obrazaca, zaključili smo o temeljnim mikroevolucijskim procesima koji djeluju u ispitivanoj populaciji s posebnim naglaskom na disperziju. Naši rezultati su pokazali značajnu prostornu genetičku strukturu i agregaciju jedinki unutar uzorkovane populacije. Na temelju prostorne genetičke strukture, srednja vrijednost disperzije unutar populacije je procjenjena u rasponu između 53 i 76 cm, potvrđujući ograničene sposobnosti disperzije ove vrste. Analiza srodstvenih odnosa na ovim uzorcima pokazala je složenu razinu odnosa, potvrđujući višestruko parenje između genetski srodnih kolonija upućujući na pojavu parenja u srodstvu. Naši rezultati proširuju prethodna saznanja, ukazujući da su populacije *C. rubrum* zatvorene i da lokalni procesi imaju središnju ulogu u njihovoj biologiji, što ima važne implikacije za očuvanje crvenog koralja.

(51 stranica, 12 slika, 5 tablica, 94 literaturnih navoda, jezik izvornika: engleski)
Rad je pohranjen u Središnjoj biološkoj knjižnici
Ključne riječi: *Corallium rubrum*, disperzija, genetički pomak, srodstvena struktura, prostorna genetička struktura

Voditelj: Dr. sc. Jean-Baptiste Ledoux

Suvoditelj: Dr. sc. Ana Galov, izv. prof.

Neposredni voditelj: Dr. sc. Silvija Kipson

Ocjenitelji: Dr. sc. Ana Galov, izv. prof.

Dr. sc. Tatjana Bakran-Petricioli, izv. prof.

Dr. sc. Petra Korać, izv. prof.

Rad prihvaćen: 04.05.2018.

TABLE OF CONTENTS

1. INTRODUCTION 1

2. THE OBJECTIVES OF THE STUDY 8

3. STUDY AREA AND SAMPLING 9

4. MATERIALS AND METHODS 11

4.1. DNA extraction and microsatellite genotyping 11

4.2. Quality control and identification of multi-sampled individuals 12

4.3. Stage-class definition 12

4.4. Spatial distribution of red coral colonies within population 12

4.5. Genetic diversity analyses 13

4.6. Linkage disequilibrium and Hardy–Weinberg equilibrium 13

4.7. Genetic homogeneity of the sample 14

4.8. Pattern of genetic structure 14

4.8.1. Temporal pattern of genetic structure 14

4.8.2. Spatial pattern of genetic structure: isolation by distance between individuals 14

4.8.3. Pattern of kinship structure and parentage analyses 15

4.9. Inference of two demographic parameters: the 'neighbourhood size' and the gene dispersal estimates 16

5. RESULTS 17

5.1. Stage-class definition 17

5.2. Spatial distribution of red coral colonies within population 17

5.3. Genetic diversity analyses, linkage disequilibrium and Hardy–Weinberg equilibrium 18

5.4. Genetic homogeneity of the sample 20

5.5. Pattern of genetic structure 21

5.5.1. Temporal pattern of genetic structure 21

5.5.2. Spatial pattern of genetic structure: isolation by distance between individuals 21

5.5.3. Pattern of kinship structure and parentage analyses 22

5.6. Inference of two demographic parameters: the 'neighbourhood size' and the gene dispersal estimates 27

6. DISCUSSION 28

7. CONCLUSIONS 32

8. REFERENCES 33

9. APPENDICES 43

10. BIOGRAPHY 51

1. INTRODUCTION

Coastal marine ecosystems are among the most ecologically and socio-economically vital systems on the planet (HARLEY ET AL., 2006), yet highly threatened by direct and indirect effects of human activities, such as overexploitation, habitat loss and degradation, eutrophication, pollution, introductions of exotic species and climate change (HALPERN ET AL., 2008), resulting in profound structural and functional changes (WALTHER ET AL., 2002). The Mediterranean Sea is considered marine biodiversity hotspot, harbouring around 13 200 species, which correspond to approximately 5% of the total known recent marine species while covering less than 0.8% of the total world ocean area (COLL ET AL., 2010). Within the Mediterranean marine habitats, coralligenous assemblages are one of the most important, as they exhibit high species richness, harbouring around 20% of Mediterranean species (BALLESTEROS, 2006). Because of their ecological, aesthetic and economic value, they have been identified as Mediterranean priority habitats by the EU Habitats Directive (92/43/CE). Coralligenous outcrops are hard bottoms of biogenic origin. They exhibit great structural complexity. Besides coralline red algae, as the main coralligenous builders, species that characterize coralligenous communities are sponges, cnidarians, bryozoans and tunicates (BALLESTEROS, 2006). Most of these species are long lived, and their slow growth and overall slow population dynamics, make coralligenous outcrops exceptionally vulnerable to anthropogenic disturbances (BALLESTEROS, 2006; CEBRIAN ET AL., 2012). Long-lived, coralligenous-habitat-forming species, play a key role in structuring and functioning of community (GARRABOU AND HARMELIN, 2002). These species create, modify and maintain habitat, through their trophic activity, biomass and perennial biogenic structures. They increase structural complexity by forming three-dimensional structures, therefore directly enhance biodiversity through the provision of microhabitats, niches and shelters to other species (GILI AND COMA, 1998; ROSSI ET AL., 2013). Three-dimensional structures which these habitat constructors create, are crucial for the existence of the multitude of associated fauna and flora and provide essential areas for fishes and mobile invertebrates for feeding, spawning, breeding and nursery (GRAHAM AND NASH, 2013). Declines in the abundance of habitat-forming species can therefore lead to a rapid fragmentation in community structure with significant impact on the ecosystem functioning (HUGHES, 1994; PONTI ET AL., 2014). The impact of positive temperature anomalies linked to climate change has been related with an increase of mass mortality events (MMEs) of marine invertebrates, mainly reported in the Western Mediterranean Sea, with the

two largest MMEs observed in 1999 and 2003 (CERRANO ET AL., 2000; GARRABOU ET AL., 2001, 2009). Due to the high levels of mortality observed, one of the main consequences of these mortality events is a decrease of population density of impacted species with potentially strong consequences for the dynamics and evolution of these species (GARRABOU ET AL. 2009). According to scenarios available for the Mediterranean basin for the end of this century, it will undergo one of the largest changes in climate worldwide with the occurrence of hot extremes increasing by 200 to 500% throughout the region (DIFFENBAUGH ET AL., 2007; IPCC 2007) questioning therefore the future of coralligenous.

The precious red coral, *Corallium rubrum* has a crucial role as one of the key engineering species inhabiting coralligenous outcrops (KIPSON ET AL., 2011). *C. rubrum* (Anthozoa, Octocorallia) is colonial, modular organism (Figure 1; HARPER AND WHITE, 1974). Based on its modular growth, red coral forms treelike three-dimensional structures (Figure 2; ROSSI ET AL., 2013).

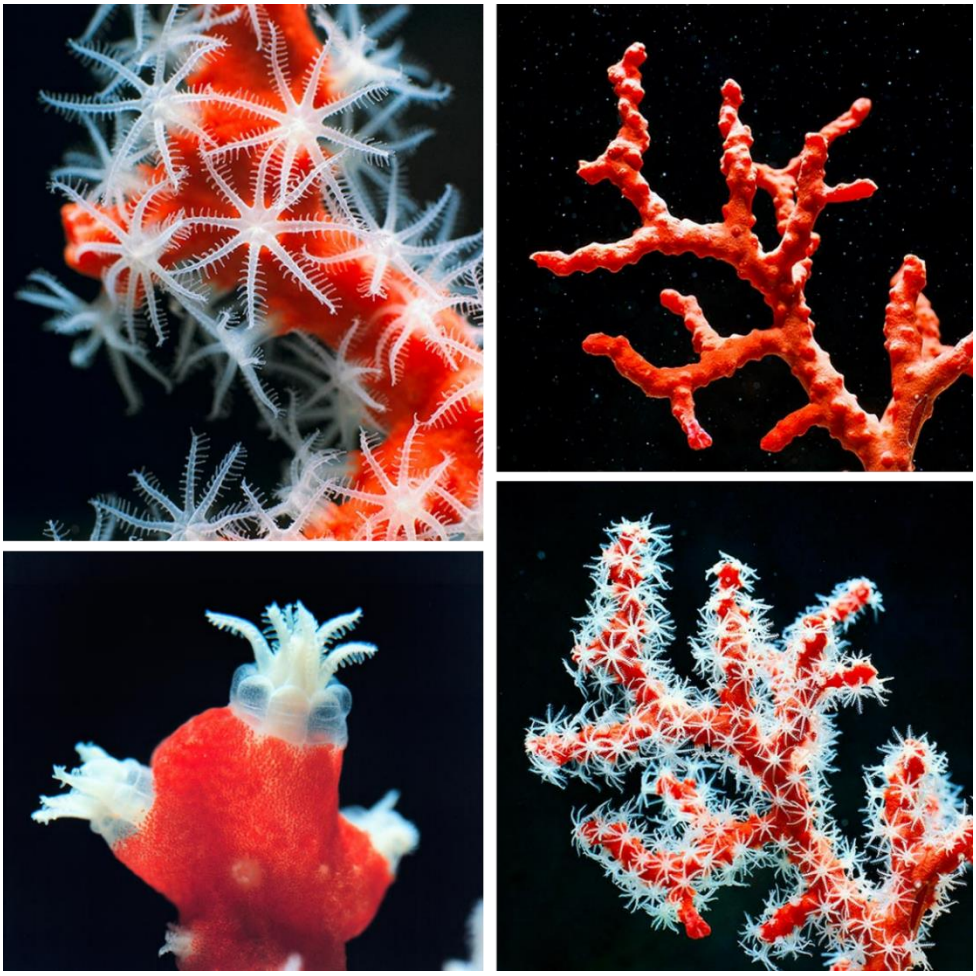

Figure 1. The red coral, *Corallium rubrum*: (Right) The polyps, passive filtrators, retreat in case of danger into the coenosarc, the spongy tissue hosting them, then get out again hunting plankont. Colony is characterized by branching morphology. (Left) Closeup of opening polyps at the end of which are distinguished 8 tentacles reaching 5 mm. Taken and modified from http://www.photomazza.com.

Figure 2. Large overhanging wall with red coral population from Marseille. Taken from Ledoux, 2010.

This is a sessile modular suspension feeder with an arborescent growth form which can live for up to 100 years (MARSCHAL ET AL., 2004). It is endemic to the Mediterranean Sea and neighbouring Atlantic rocky shores (FAO, 2018). Red coral is a sciaphilous species which dwells in heterogeneous habitats, as it can be found below 10 m to depths greater than 1000 m (ROSSI ET AL., 2008; COSTANTINI ET AL., 2010; TAVIANI ET AL., 2010; KNITTWEIS ET AL., 2016), but it is more commonly found between 30 and 200 m (CAU ET AL., 2016). Red coral distribution is fragmented. It has extremely slow mean annual growth rate of basal diameter, varying between 0.23 – 0.35 mm $year^{-1}$ (Figure 3; MARSCHAL ET AL., 2004; PRIORI ET AL., 2013; BRAMANTI ET AL., 2014; BOAVIDA ET AL., 2016) and can reach more than 50 cm in height (GARRABOU AND HARMELIN, 2002).

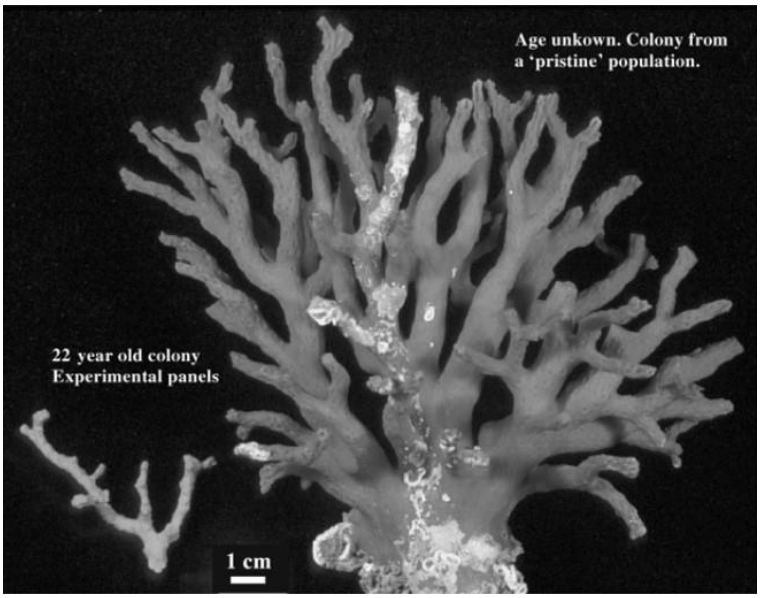

Figure 3. A 20-year-old red coral colony collected in 2000 from the experimental panels and a colony from a pristine site (age unknown) collected at the same depth in 1962 from the private collection. Taken from Garrabou and Harmelin (2002).

Red coral is a gonochoric, iteroparous brooder that undergoes internal fertilisation and reproduces annually during late spring – early summer (VIGHI, 1972; SANTANGELO ET AL., 2003; TSOUNIS ET AL., 2006). It broods larvae internally, within the female polyps for about 30 days. After that embryonic period, the mature larvae are released from late June and throughout July. They survive only a few days (4-12) and have limited dispersal capabilities (WEINBERG, 1979; BRAMANTI ET AL., 2005). The red coral has a balanced sex-ratio (BRAMANTI, 2014) and reaches sexual maturity at relatively small sizes (about 2 mm in diameter and 30 mm in height) which corresponds to ages between 7 and 10 years old (TORRENTS, 2005), but at least 20 years are needed to reach high reproductive potential (GARRABOU AND HARMELIN, 2002). Old and large colonies produce almost 300 times more larvae than small colonies (PRIORI ET AL., 2013), suggesting that there should be large differences in larval output between populations with different size and age structures. However, small colony size at first reproduction may be the main reason for the persistence of red coral populations despite to the millennia of harvesting pressure (TORRENTS ET AL., 2005). Red coral, owing to its larval biology, life history and patchy distribution, is assumed to be a poor disperser with mostly self-seeded populations, and with higher levels of population genetic differentiation than in broadcast spawning species (UNDERWOOD ET AL., 2009; but see SERRANO ET AL., 2016). Magnitude of loss of large red coral colonies due to overexploitation for its use in jewellery resulted in significant shifts in the demographic structure of shallow red coral populations in the Mediterranean Sea (LINARES ET AL., 2010). Therefore, shallow populations are generally characterized by small colonies (~ 3 cm in height) of a relatively high density (~ 500 colonies m^{-2}) (GARRABOU ET AL., 2017), making populations look more like grasslands than like forests (ROSSI ET AL., 2008). Despite this decrease, demand is increasing, fuelling exploitation of deep stocks and illegal poaching (TSOUNIS ET AL., 2013). This important fishing pressure can cause the loss of genetic variation, which could have important consequences on the long-term evolution of the red coral populations (PINSKY AND PALUMBI, 2014). Moreover, natural (e.g., increase of sedimentation, parasites, alien species) and anthropogenic stressors (e.g., harvesting, habitat loss and fragmentation, climate change, ocean acidification) affect red coral populations along its entire bathymetrical distribution. For instance, recent mass mortality events already affect its shallow (5–60 m) populations with until 80% mortalities in some populations (GARRABOU ET AL., 2001). Thus, slow growth rates and high longevity suggest that full recovery from damage can take decades for the red coral (GARRABOU AND HARMELIN, 2002). Given its ecological, economical, aesthetic and cultural value (BRAMANTI ET AL., 2011), red coral has been protected by three

international conventions (Barcelona, Berne and the European Habitat Directive). Recently, General Fisheries Commission for the Mediterranean (Recommendation GFCM /35/2011/2) has recommended the full protection from fishing of populations at depth less than 50 m until scientific studies and promoted a minimum harvestable size (7 mm of colony basal diameter) corresponding to an age of about 30–35 years. However, these management measures do not take into account population genetics and dynamics of the red coral. Thus our ability to infer the eco-evolutionary processes shaping and maintaining spatial pattern of genetic diversity of the red coral is key to propose efficient conservation policies (HENDRY ET AL., 2010) and hence for the conservation of shallow populations of *C. rubrum*.

If we define microevolution as changes in the gene (or allelic) frequencies within a population over generations (HARTL AND CLARK, 1989), than population genetics would be at the very heart of evolutionary biology (TEMPLETON, 2006). Random genetic drift and gene flow are two of the main evolutionary forces that change gene frequencies. Genetic drift is stochastic fluctuation of allelic frequencies from one generation to the other, through the random selection of alleles to be combined into progeny (PALUMBI, 2003) and connectivity (i.e. gene flow) refers to the movement of individuals between populations (PALUMBI, 2003) and their residence for enough time to contribute to the gene pool of the new population ('migration' in the population genetics) (LOWE AND ALLENDORF, 2010). The strength of genetic drift in a population is determined by effective population size (*Ne*), which can be defined as the number of individuals actually contributing to the next generation (FRANKHAM, 1995) and is one of the fundamental parameters in population genetics (HARE ET AL., 2011). When *Ne* decreases, drift erodes genetic variation, eventually leading to the loss of rare alleles and fixation of others (possibly deleterious ones). Also, as *Ne* declines, the effectiveness of selection reduces, because directionless changes in gene frequency driven by genetic drift progressively start to have stronger effect over directed changes driven by selection (HARE ET AL., 2011). Loss of genetic diversity can decrease population viability and adaptive potential under environmental change. Thus, small and isolated populations are at major risk of extinction due to strong impact of genetic drift and inbreeding (FRANKHAM, 2005). Harmful effects of genetic drift and inbreeding can be offset by gene flow which replaces alleles lost due to drift, increases genetic variation, reduces inbreeding and stochastic variation in small populations (STOCKWELL ET AL., 2003). Thus the extent to which populations are connected by dispersal is fundamental to the ecological and evolutionary processes, and protecting patterns of connectivity allows for population persistence and recovery from disturbance (UNDERWOOD ET

AL., 2013). Therefore, the integration of eco-evolutionary analyses at contemporary timescales is necessary and highly valuable for conservation planning (ARIZMENDI-MEJÍA ET AL., 2016). For sessile and sedentary benthic invertebrates, larval phase is effectively the only time dispersal within and between populations occurs and in general, correlation between dispersal of larvae and distance is expected, which forms a basis for IBD pattern also called fine-scale spatial genetic structure (FSGS). FSGS is defined as non-random spatial distribution of genotypes within the red coral population and the most prevalent cause for the FSGS is the formation of local pedigree structures as a result of limited gene dispersal. Focusing on IBD model, parent–offspring dispersal distances rate can be accurately inferred from genetic data (VEKEMANS AND HARDY, 2004).

Genetic structuring among red coral populations was first described using allozymes (ABBIATI ET AL., 1993, 1997). These studies demonstrated significant genetic differentiation at a spatial scale of tens of kilometres. At shorter distances (about 200 m), no significant genetic structuring was observed, due to low mutation rate and low polymorphism of allozyme markers. Development of species-specific microsatellite loci (COSTANTINI AND ABBIATI, 2006; LEDOUX ET AL., 2010b), which has higher levels of polymorphism, allowed refining the characterization of the pattern of genetic structure. Significant genetic differentiation was observed between populations separated by tens of meters demonstrating the low connectivity in the red coral (COSTANTINI ET AL., 2007a; LEDOUX ET AL., 2010a). At a scale of hundreds of kilometres, pattern of genetic structure results from the combination among IBD and regional genetic clusters (AURELLE ET AL., 2011; AURELLE AND LEDOUX, 2013; LEDOUX ET AL., 2010b).

These studies also revealed significant deviations from Hardy-Weinberg equilibrium towards heterozygote deficiencies in all red coral populations likely due to the occurrence of null alleles, temporal or spatial Wahlund effect and biparental inbreeding (i.e. mating between genetically close relatives) (COSTANTINI ET AL., 2007a ; LEDOUX ET AL., 2010a). Accordingly, studies at fine spatial scale (< 1m) were conducted (COSTANTINI ET AL., 2007a; LEDOUX ET AL., 2010a). More particularly, the FSGS was studied among red coral colonies over half a square meter (LEDOUX ET AL., 2010a). In this study of genetic structuring at a very fine scale, Ledoux *et al*. (2010a) revealed for the first time significant spatial and temporal genetic structure between colonies of the red coral over half a square metre. This study was focused on a population showing the demographic structure of an impacted population with high density of low size colonies in contrast to the population studied in the present work, which showed a low density of

relatively high size colonies. Based on isolation by distance analyses, Ledoux *et al*. (2010a) estimated the mean effective dispersal within a population to range between 20 and 30 cm and a small 'neighbourhood size' of 75 individuals. The sibship analyses revealed a complex half-sib family structure with 78.9 % of the nonmature colonies and 84.2 % of the recently mature colonies linked by half-sib relation, suggesting that breeding units in the red coral are highly restricted in space and are composed of related individuals. These results were also in agreement with previous studies that found high levels of genetic structuring in the red coral at spatial scales of 10s to 100s of kilometres (COSTANTINI ET AL., 2007a,b; LEDOUX ET AL. 2010b) and demonstrated that the red coral is a poor disperser species with self-seeded populations. It was the first time that such a complex pattern of kinship structuring has been characterized in a sessile marine species. In addition, the occurrence of several parent-offspring dyads demonstrated that self-recruitment was an important process in the dynamics of the study population. These results were obtained in a population impacted by various anthropogenic pressures and thus characterized by a particular demographic structure with high density of low size colonies. Accordingly, the generalisation of this study is not straightforward and there is a need to study other populations with different demographic characteristics in order to improve our understanding of red coral population dynamics.

2. THE OBJECTIVES OF THE STUDY

The major goal of this study was to follow the characterization of the patterns of fine-scale spatial and temporal genetic structure in the red coral focusing on a protected population (i.e. showing different demographic characteristics). Based on these patterns, the aim was to infer underlying microevolutionary processes acting in the study population with particular emphasize on dispersal. To achieve this aim, a multidisciplinary approach was developed by combining population genetics, ecology and photogrammetry, and focusing on a shallow population of the Mediterranean red coral, *Corallium rubrum*, belonging to the marine reserve of Scandola (Corsica, France). 107 georeferenced red coral colonies were sampled over an area of two square meters in the Passe Palazzu and genotyped with 9 microsatellite loci to address following objectives:

- to assess the spatial distribution of mapped red coral colonies in the study population
- to characterize the pattern of spatial genetic structure
- to decompose the IBD pattern among juveniles and adults
- to infer the demographic parameters linked to local dispersal
- to characterize the kinship structure among the colonies
- to test for temporal genetic differentiation among juveniles and adults and describe the mating system in the study population

3. STUDY AREA AND SAMPLING

This study was carried out in the Passe Palazzu, France (42° 22’ 47.64’’N, 8° 32’ 51.29’’E; Figure 4), in the marine protected area of the Scandola Natural Reserve located in the NW Corsica. In October 2016, the sampling of *Corallium rubrum* colonies was conducted by scuba diving at a depth of 14 m in an area of approximately 2 m^2 (4.9 x 0.38 m) along a permanent transect.

Figure 4. Location of the Passe Palazzu where the sampling of the red coral colonies was conducted.

The area where our colonies were sampled from, is a typical population from marine protected area (Scandola) consisting of a low density (approximately 50 colonies.m^{-2}) of relatively large colonies (around 5 cm in height). Due to demographic characteristics of our population, georeferenced sampling at the individual level was possible. Underwater photographs (each covering 400 cm^2) were used to map the colonies. The photographs were analysed with photogrammetric methods (ROYER ET AL., 2018) and the accurate position of each colony was determined as well as pairwise distances between colonies (Figure 5). 107 red coral fragments were sampled, preserved in 95% ethanol and stored at -80^{0}C until DNA extraction.

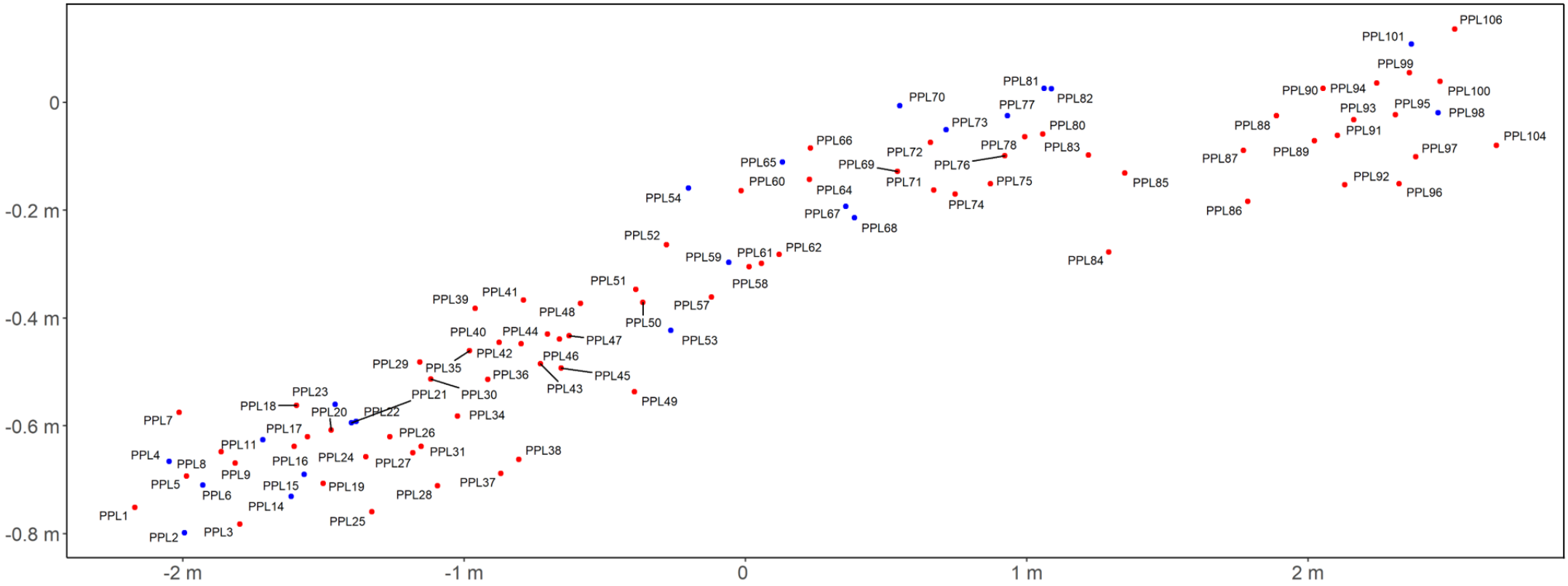

Figure 5. Map of the sampled colonies of *Corallium rubrum* in the study area. Only the 94 genetically different individuals, corresponding to 72 mature (•) and 22 nonmature (•) colonies, are shown.

4. MATERIALS AND METHODS

4.1. DNA extraction and microsatellite genotyping

Total genomic DNA was extracted from 107 individuals using a salting out procedure adjusted from Miller *et al*. (1988) (see Appendix 1 for details). All samples were genotyped using 9 microsatellite loci: Mic13, Mic20, Mic22, Mic23, Mic24, Mic25, Mic26, Mic27 and COR46*bis* previously published (LEDOUX ET AL., 2010). For amplifying loci, 3 multiplex polymerase chain reactions (mPCRs) were performed, each targeting different loci: mPCR1 (Mic13, Mic20, Mic26), mPCR2 (Mic24, Mic25, Mic27), mPCR3 (Mic22, Mic23). COR46*bis* was amplified separately. mPCR amplifications were performed in a final volume of 10 µL containing 1 µL of DNA, 5.5 µL of Master Mix, 1.1 µL of Primer Mix and 3.4 µL of Milli-Q water. PCR amplification of the COR46*bis* was carried out in a final reaction volume of 10 µL containing 2 µL of DNA, 1 µL of *Taq* DNA Polymerase PCR Buffer, 0.5 µL of $MgCl_2$, 0.2 µL of dNTPs, 0.05 µL of *Taq* Polymerase, 5.25 µL of Milli-Q water and 0.5 µL of each primer. The forward primer of each locus was fluorescently labelled. mPCR reactions were done as follows for all loci except COR46*bis*: 95°C for 15 min followed by 30 cycles at 94°C for 30 s, annealing temperature for 1 min 30 s and 72°C for 1 min. The final step was 60°C for 30 min. Amplification of COR46*bis* was done as follows: 94°C for 3 min, 28 cycles at 94°C for 30 s, 53°C for 30 s and 72°C for 30 s. The final holding was 72°C for 20 min. PCR products were genotyped on an ABI3730XL DNA Sequencer with GeneScan LIZ 600 (Applied Biosystems) internal size standard at the GenoScreen sequencing facility (Lille, France; https://www.genoscreen.fr/fr/). Alleles were scored using STRand version 2.4.109 (TOONEN AND HUGHES, 2001; UC Davis Veterinary Genetics Laboratory; http://www.vgl.ucdavis.edu/STRand). Genotyping accuracy was evaluated by amplifying and genotyping replicates.

4.2. Quality control and identification of multi-sampled individuals

MICRO-CHECKER v.2.2.3 (VAN OOSTERHOUT ET AL., 2004) was used to check for scoring errors due to stuttering, null alleles or large allele dropout. Because some colonies were closely related in space, GIMLET v1.3.3 (VALIÈRE, 2002) was used to look for duplicate genotypes due to putative multiple sampling of the same individual and to estimate the unbiased probability of identity ($P_{ID;}$ KENDALL AND STEWART, 1977) that two individuals in the sample will by chance have the same multilocus genotype. The unbiased probability of identity between two different multilocus genotypes was 6.13×10^{-11}. Therefore, two multilocus genotypes shared by four colonies were considered as sampling errors and only one of each repeated genotype was retained. Additionally, one genotype containing more than three null alleles was eliminated. Thus, the following analyses were conducted with a final data set of 94 different multilocus genotypes.

4.3. Stage-class definition

The maximum diameter and height were measured for each colony to define their reproductive status (mature vs. juvenile). These photogrammetric methods were carried out with Arpenteur 6.0 (GRUSSENMEYER and DRAP, 2000). Over the 94 colonies, 72 were considered as adults and 22 as juveniles. Thus two different datasets were considered: one including all the individuals and one considering adult and juvenile stage-classes as two distinct populations.

4.4. Spatial distribution of red coral colonies within population

To assess the spatial distribution of mapped red coral colonies in the study population, the univariate O-ring statistic O(*r*) (WIEGAND AND MOLONEY, 2004, 2014) was calculated. O(*r*) gives the expected number of points (that is, red coral colonies) in a ring at distance *r* from an arbitrary point. O(*r*) was calculated considering concentric rings of a constant width of 0.1 m. To test the significance of O(*r*) for each *r*, 95% simulation envelopes associated to the null

model of complete spatial randomness were generated using the fifth lowest and fifth highest value of 199 Monte Carlo simulations of the complete spatial randomness-null model. O(*r*) values above and below the envelope indicate significant spatial aggregation and repulsion compared with a complete spatial randomness pattern. All calculations and simulations were conducted using the program PROGRAMITA (WIEGAND AND MOLONEY, 2004, 2014).

4.5. Genetic diversity analyses

Frequencies of null alleles were estimated by the Expectation Maximization (EM) algorithm (DEMPSTER EL AL., 1977) implemented in FreeNA (CHAPUIS AND ESTOUP, 2007) for each locus. The total number of alleles (N_a), observed (H_o) and unbiased heterozygosity (H_e; NEI, 1973) were calculated for each locus using FSTAT v.2.9.3 (GOUDET, 2001).

In addition, observed (H_o), unbiased heterozygosity (H_e; NEI, 1973) and rarefied allelic richness (*AR*) were computed for the two datasets. Allelic richness is dependent on sample size. The rarefaction method (PETIT ET AL., 1998) allows evaluation of the allelic richness independent of the sample size. For the whole dataset, allelic richness was calculated based on the sample size of 68 individuals, corresponding to the minimum number of individuals observed at one locus. When considering juveniles and adults separately, allelic richness was calculated based on the same standardized sample size of 14 individuals.

4.6. Linkage disequilibrium and Hardy–Weinberg equilibrium

GENETIX v.4.05 (BELKHIR ET AL., 2004) was used to test for genotypic linkage disequilibrium for each pair of loci with a permutation procedure (N = 1000) considering the whole dataset. Departure from panmixia was tested for each locus and for the whole sample using the score test for heterozygote deficiency in GENEPOP v.4.6.9 (ROUSSET, 2008). Significance was addressed by a Markov Chain (MC) algorithm (GUO AND THOMPSON, 1992), with default parameters. The *f* estimator of F_{IS} (WEIR AND COCKERHAM, 1984) was computed for each locus separately and for all loci in each dataset using GENETIX.

4.7. Genetic homogeneity of the sample

In order to identify any potential genetic structure within the sample, Bayesian clustering method implemented in STRUCTURE v.2.2 (PRITCHARD ET AL., 2000) that infers the number of genetic clusters (*K*) from the individuals' genotypes was used. Individuals are assigned to population(s) in a way that, within population, Hardy-Weinberg equilibrium and linkage equilibrium are maximized. Admixture model (i.e. individuals may have mixed ancestry) was used under assumption of correlated allele frequencies between clusters (FALUSH ET AL., 2003), and the recessive allele option was used to deal with null alleles. Ten replicated runs were computed for each *K* (*K* = 1 - 5) to check the consistency of the results with 500 000 burn-in iterations followed by 200 000 retained iterations. The outputs of STRUCTURE analysis were collated and visualized with the STRUCTURE HARVESTER Web v0.6.94 (EARL AND VON HOLDT, 2012). The *K* value that better fit the dataset was inferred based on the plot of *LnP*(*D*) (the logarithm of the likelihood of observing the data) as a function of *K*.

4.8. Pattern of genetic structure

4.8.1. Temporal pattern of genetic structure

In order to look for temporal structure, genotypic differentiation between two stage-classes: adults and juveniles was tested using an exact test in GENEPOP. Significance of F_{ST} values was evaluated using MC algorithm with default parameters.

4.8.2. Spatial pattern of genetic structure: isolation by distance between individuals

Pattern of isolation by distance was tested using regression analyses. Genetic distance between every pair of individuals was estimated with Rousset's genetic distance $\hat{e}$ (WATTS ET AL., 2007), as implemented in GENEPOP. Then the obtained values were regressed on the natural logarithm of the geographical distance between individuals (*ln(d)*) following Rousset (2007). The significance of the regression was tested using a Mantel test with 1000 permutations.

4.8.3. Pattern of kinship structure and parentage analyses

In order to further examine fine-scale spatial genetic structure, Loiselle's kinship coefficient (F_{ij}) (LOISELLE ET AL., 1995) was calculated for each pair of individuals separated by progressively increasing distances from 0 to 6 m. The average value of the kinship coefficient was computed over all pairs of individuals within each distance interval. The kinship coefficient (F_{ij}) was chosen as a pairwise estimator of genetic relatedness, as it is a relatively unbiased estimator with low sampling variance (VEKEMANS AND HARDY, 2004). Significance was determined by comparing the observed values with corresponding frequency distributions obtained after 1000 random permutations of the data (i.e. permutations of individual locations among all individuals within each distance interval). These analyses were first conducted considering the whole dataset and then analyses were limited to individuals of adults, juveniles and adult-juvenile pairs. Significance of the linear regression slope was calculated with 1000 permutations of locations, as well. All calculations were made using SPAGeDi 1.4 (HARDY AND VEKEMANS, 2002).

Parentage analyses between individuals, i.e. sibship and parentage structure within the sample, were conducted using the maximum likelihood approach implemented in COLONY v.2.0 (WANG AND SANTURE, 2009; JONES AND WANG, 2010). The method assigns parentage and sibship among individuals using their multilocus genotypes while accounting for genotypic errors. Four different categories of relationships were considered: parent-offspring, full-sib, half-sib or unrelated. For the 22 colonies belonging to the juveniles, the remaining 72 mature colonies were considered as candidate male and female parents. The analysis was run three times with three different random seed numbers to check the robustness of our results.

Geographical distance for each obtained relationship category was compared using a nonparametric Kruskal – Wallis test.

4.9. Inference of two demographic parameters: the 'neighbourhood size' and the gene dispersal estimates

Under Wright's two-dimensional IBD model, neighbourhood size *Nb*, is considered to be equal to $4\pi D_e \sigma^2_g$, where D_e is effective (breeding) population density and σ^2_g is the mean square parent-offspring distance (VEKEMANS AND HARDY, 2004). Following Watts *et al*. (2007) *Nb* can also be derived from the slope of the regression line between $\hat{e}$ and *ln(d)*: $Nb = 1 / b_{L(d)}$. Therefore, *Nb* was computed from the regression slope based on the whole data set and estimated values of D_e were used to calculate σ_g. D_e can be approximated as $D_e = (N_e / N) \times D$ (VEKEMANS AND HARDY, 2004), where *D* is the census density of mature individuals, and N_e and *N* are the effective and the census population sizes, respectively. In this study, 94 different colonies were sampled on an area of 2 m^2 and therefore, approximated density of the site was 47 colonies x m^2. 77% of those colonies were considered sexually mature with a resulting density of 36 colonies x m^2. Because N_e / N is unknown for *Corallium rubrum*, two different values were used considering that all or only 50% of the mature colonies were involved in the reproductive effort (i.e. $D_e = D$ = 36 colonies x m^{-2} or $D_e = 0.5 \times D$ = 18 colonies x m^{-2}).

For multiple tests, significance levels were corrected using a false discovery rate (FDR) correction (BENJAMINI AND HOCHBERG, 1995).

5. RESULTS

5.1. Stage-class definition

For majority of the colonies, diameter could not be measured accurately enough. Therefore, colonies were divided based on the difference in size. Colonies higher than 30 mm were considered mature and the rest were assigned to juveniles, following Torrents *et al*. (2005). Height measurements for 7 colonies (7%) could not be obtained due to their complex shapes, their position to other colonies, substrate ruggedness and a lack of adequate pictures needed to perform photogrammetric measurements. In those cases, the reproductive status was assessed visually relative to the measured colonies. In total, 72 colonies (77%) were considered mature (mean height size ± s.d. = 59.5 ± 18.3 mm) and potential parents for the rest 22 juvenile colonies (mean height size ± s.d. = 23.1 ± 7 mm) (Appendix 2; Figure 6).

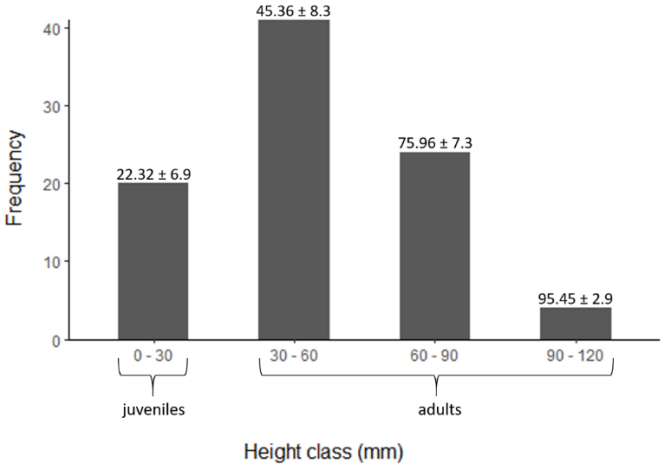

Figure 6. Size structure distribution of red coral colonies sampled at the Passe Palazzu, Corsica. The largest colony measured was 10 cm high and the smallest was 0.5 cm. Numbers above the bins represent mean (± s.d.) values of maximum heights (mm) in every height class.

5.2. Spatial distribution of red coral colonies within population

The O-ring statistic O(*r*) showed significant spatial aggregation of red coral colonies up to *r* = 30 cm in our study population (Figure 7).

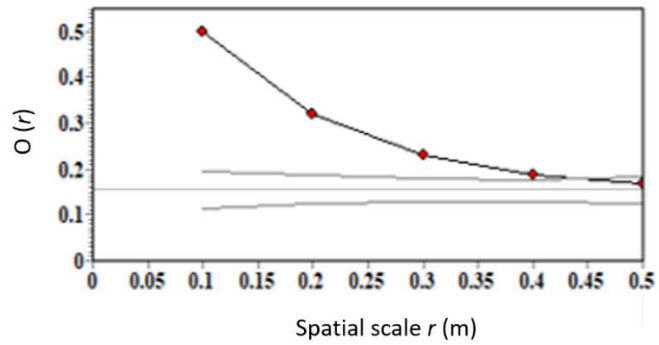

Figure 7. Spatial structure of total red coral colonies measured using the O-ring statistic (O(*r*)). Closed circles represent mean O(*r*) for an annulus of radius *r* with 0.1-m lags. Horizontal line indicates average intensity of the point pattern and thick lines indicate 95% confidence envelopes under the null hypothesis of random spatial structure.

5.3. Genetic diversity analyses, linkage disequilibrium and Hardy–Weinberg equilibrium

The raw genotype data can be found in the supplementary material (Appendix 3). Micro-Checker analysis found no evidence for scoring error due to stuttering and large allele dropout in the whole data set. Null allele frequencies ranged from 0.000 for Mic23 and Mic26, to 0.253 for Mic27, with a mean value of 0.079 per locus. Although three pairs of loci were out of linkage equilibrium, none of the 36 combinations was significant after FDR correction at 0.05. Allelic richness for the whole dataset, based on the sample size of 68 individuals, was approximately 12 alleles. All loci were polymorphic with a total number of alleles ranged between 4 for Mic13, to 26 for Mic27, with a mean value of approximately 12 alleles per locus. The observed and unbiased expected heterozygosity varied between 0.255 (Mic13 and Mic20) and 0.915 (Mic24), with a mean value of 0.574 over the whole dataset, and between 0.295 (Mic20) and 0.929 (Mic24), with a mean value of 0.703 for the whole dataset, respectively. The inbreeding coefficient F_{IS} is measure of reduction in heterozygosity in a population when compared to Hardy–Weinberg expectation and exhibits values ranging from -1 to +1, with values close to zero being expected under random mating. Locus values of the *f* estimator of inbreeding coefficient F_{IS} varied between -0.073 for Mic23, to 0.559 for Mic27. Our positive values indicated departure from Hardy–Weinberg equilibrium towards heterozygote deficiency and significant deviation from panmixia was observed for five of the nine loci after FDR correction. The multilocus value was equal to 0.184 and according to global test across loci, deviation from panmixia was significant (P = 0.000). Detailed results for each locus are shown in Table 1.

Table 1. Primer sequences, repeat motif, PCR conditions and genetic characteristics of 9 amplified polymorphic microsatellites in *Corallium rubrum*.

Locus name	Primer sequence (5' - 3')	Repeat motif	Number of cycles	Ta (^{0}C)	Size range (bp)	N_a	H_o	H_e	*f*	*r*	Genbank accession number
Mic13	F: NED_CTTTGATTGGCCCTGATGTAA R: GCCAGGAAAGAATTGGGTATATTA	$(AC)_2$ A (AC) G $(AC)_3$ TA $(AC)_7$	30	59	126 - 141	4	0.255	0.417	0.387***	0.138	GQ169280
Mic20	F: 6-FAM_CACGTGATTGACGAAAACATTC R: TGTCGGGAAATTGTTCACTGTA	$(CA)_8$	30	59	198 - 286	6	0.255	0.295	0.136*	0.038	GQ169281
Mic22	F: VIC_CGAGCGAGGGAAATTAATAGG R: GATGTAATTGTCGCGCATTG	$(GT)_{16}$	30	56	153 - 190	6	0.462	0.559	0.172	0.044	GQ169282
Mic23	F: VIC_GATCTCTGACTGAATGGTATTGG R: CCTGGCTACGTCCCTGACT	$(GT)_{14}$	30	56	93 - 143	10	0.862	0.803	-0.073	0.000	GQ169283
Mic24	F: NED_ TCGAGCACTTCCTTGGTAGC R: TGAATTCCATACACCCACTGC	$(CA)_{18}$	30	59	145 -312	20	0.915	0.929	0.015	0.002	GQ169284
Mic25	F: 6-FAM_GCAAGGTAAAATGATGTAGTCTGG R: GATCGCACTAAATCTTAATAGTGTTCC	$(GTTT)_3$ $(GT)_{16}$	30	59	130 - 208	11	0.419	0.770	0.456***	0.199	GQ169285
Mic26	F: NED_AGGGAACAATCTTTGTTGTGC R: ATGTTTGCGGACCTACACG	$(GT)_{24}$	30	59	126 - 200	15	0.894	0.896	0.002	0.000	GQ169286
Mic27	F: 6-FAM_ GATCTCTTCGCGGATAGTCTG R: GACGGTGGGACGAACAGG	$(GT)_{30}$	30	59	140 - 536	26	0.382	0.866	0.559***	0.253	GQ169287
COR46*bis*	F: NED_TTGGGTACAAATCAAGCTACCA R: AGACCAGCGGCATCACTTT	$(GT)_{15}$	28	53	172 - 243	12	0.722	0.795	0.091*	0.037	AY726761

Abbreviations: Ta, annealing temperature; N_a, number of alleles per locus; H_o, observed heterozygosity; H_e, gene diversity (Nei, 1967); *f*, Weir and Cockerham (1984) estimator of F_{IS}; *r*, null allele frequency. Values marked with asterisks are significant at the 0.05 level after FDR correction; ***, $P = 0.000$; *, $0.01 < P < 0.05$.

Considering adults and juveniles, highly similar values of genetic diversity and inbreeding in comparison with global dataset were obtained (Table 2).

Table 2. Genetic diversity parameters of *Corallium rubrum* at the global and stage-class levels.

Dataset	N_a	*AR*	H_o	H_e	*f*	*r*
Global	12.222	11.783	0.574	0.703	0.184 ***	0.079
Adults	11.222	7.470	0.578	0.706	0.182 ***	0.075
Juveniles	8.333	7.285	0.561	0.695	0.193 ***	0.082

Abbreviations: N_a, number of alleles per locus; *AR*, allelic richness with rarefaction for a corresponding sample size of 68 individuals for global, and 14 individuals for adults and juveniles dataset; H_o, observed heterozygosity; H_e, gene diversity (NEI, 1967); *f*, Weir and Cockerham (1984) estimator of F_{IS}; *r*, null allele frequency. Presented values correspond to the mean value over all loci. Values marked with asterisks are significant; ***, $P = 0.000$.

Null allele frequencies ranged from 0.000 (Mic20, Mic23 and Mic26) to 0.273 (Mic27) for adults, with a mean value of 0.075 per locus, and from 0.000 (Mic23, Mic24, Mic26 and COR46*bis*) to 0.267 (Mic25) for juveniles, with a mean value of 0.082 per locus. Allelic richness, based on the sample size of 14 individuals, was almost the same for two stage-classes with value of approximately 7 alleles. Number of alleles ranged between 4 (Mic13 and Mic20), to 22 (Mic27) for adults, with a mean value of 11.222, and between 3 (Mic22), to 15 (Mic24) for juveniles, with a mean value of 8.333. The observed heterozygosity ranged from 0.264 (Mic13) to 0.903 (Mic24) for adults, with a mean value of 0.578, and from 0.182 (Mic20) to 0.955 (Mic24 and Mic26) for juveniles, with a mean value of 0.561. Unbiased expected heterozygosity ranged from 0.284 (Mic20) to 0.931 (Mic24) for adults, with a mean value of 0.706, and from 0.333 (Mic20) to 0.910 (Mic24) for juveniles, with a mean value of 0.695. The *f* estimator of inbreeding coefficient F_{IS} varied between -0.085 (Mic23) to 0.602 (Mic27) for adults, with a mean value of 0.182, and between -0.051 (Mic26) to 0.646 (Mic25) for juveniles, with a mean value of 0.193. Both adults and juveniles showed significant departures from Hardy–Weinberg equilibrium towards heterozygote deficiency, according to global test across loci ($P = 0.000$).

5.4. Genetic homogeneity of the sample

Considering the plot of *LnP*(*D*) as a function of *K*, no major genetic discontinuity was assumed in our sample because only one cluster was detected by Structure.

5.5. Pattern of genetic structure

5.5.1. Temporal pattern of genetic structure

Index of genetic differentiation (F_{ST}) is measure of reduction in heterozygosity in a population caused by differences in allele frequencies of individual subpopulations of which it is composed, and results from the balance between gene flow and genetic drift. It ranges from F_{ST} = 0 (no genetic differentiation) to 1 (complete genetic differentiation). In accordance with previous result, pairwise genotypic differentiation test between the adults and juveniles was very low (F_{ST} = -0.004) and not significant (P = 0.863).

5.5.2. Spatial pattern of genetic structure: isolation by distance between individuals

Regression analysis between pairwise genetic ($\hat{e}$) and geographic ($ln(d)$) distances showed highly significant correlation (P = 0.000) for the whole dataset, confirming the occurrence of an isolation by distance model (Figure 8). Adults dataset also displayed highly significant IBD pattern (P = 0.000). On the contrary, no IBD was found in the case of juveniles, but low number of juveniles should be taken into account, as it might had an influence on the statistical power of the analysis.

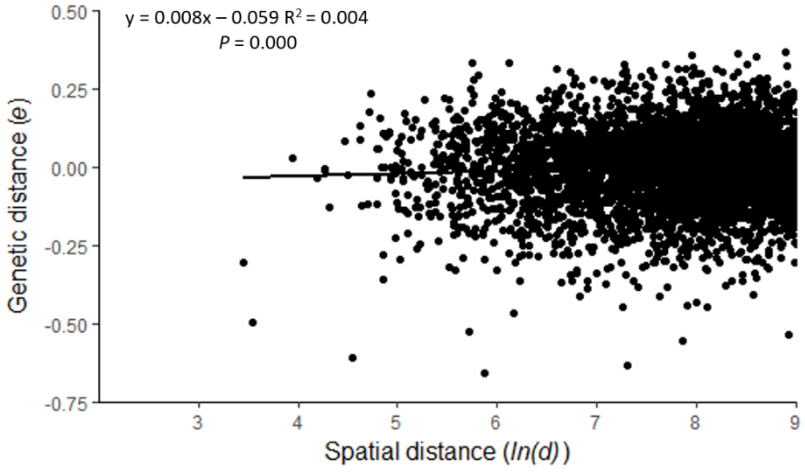

Figure 8. Linear regression between the geographical ($ln(d)$) and the genetic ($\hat{e}$) distances between pairs of colonies of *Corallium rubrum*.

5.5.3. Pattern of kinship structure and parentage analyses

Over the three runs of kinship analysis, 83 dyads in juvenile dataset were obtained, but only relationships with probability > 0.5 within the each of three runs were retained. Therefore, 7 half–sib dyads were obtained, but no full–sib or parent–offspring dyads were inferred. The resulting pedigree showed that 15 colonies were kin–related sharing one parent. This corresponds to 68% of the 22 juveniles colonies. These results demonstrated the occurrence of a half–sib family structure. The mean geographical distance (±s.d.) between those half–sib colonies was 0.88 ± 0.9 m and lower than the mean value of distance between unrelated colonies which was 1.62 ± 1.12 m (Figure 9). Nevertheless, according to Kruskal – Wallis test, geographical distances of the two relationship categories were not significantly different (H = 3; d.f. = 1; $P > 0.05$).

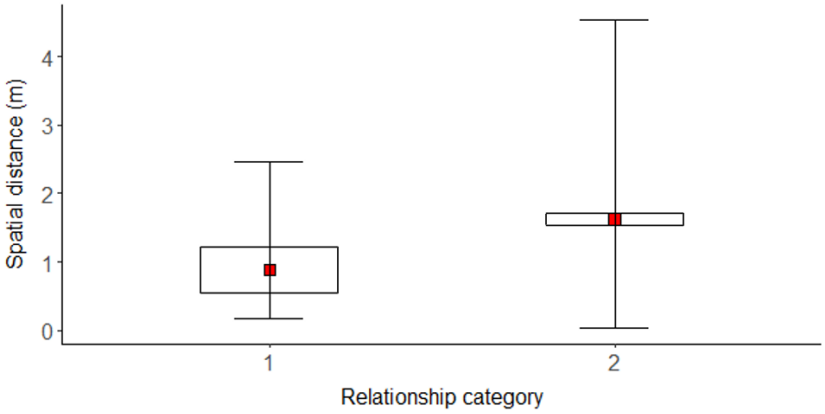

Figure 9. Mean values (▪) of distances between half–sib (1) and unrelated (2) colonies. Boxes and bars represent standard error of the mean and standard deviation, respectively.

Details of each distance class: the upper and lower limit, the number of pairs of individuals, the value and significance of average Loiselle's kinship coefficient, are shown in Table 3. For each dataset, value and significance of regression slope of pairwise kinship coefficients on the logarithm of spatial distance, are shown in Table 4.

Table 3. Average Loiselle's kinship coefficients between pairs of individuals within 14 distance classes for global, between-generation, adults and juveniles dataset. Coloured fields indicate positive kinship coefficients while distance classes differing significantly from the mean permutated kinship value are marked with asterisks: ***, $P = 0.000$; **, $P < 0.01$; *, $0.01 < P < 0.05$.

Distance class	Span (m)	Number of pairs				Average Loiselle's kinship coefficient			
		global	between-generation	adults	juveniles	global	between-generation	adults	juveniles
0	-	4371	1584	2556	231	**0.168*** **	**0.168*** **	**0.163*** **	**0.192*** **
1	0.00 - 0.50	849	278	520	51	**0.009** **	0.009	**0.010** **	-0.006
2	0.50 - 0.75	389	134	232	23	0.007	0.004	0.006	**0.037** *
3	0.75 - 0.91	227	90	133	4	0.002	0.004	0.001	0.011
4	0.91 - 1.50	789	317	440	32	0.002	0.002	0.003	-0.009
5	1.50 - 1.59	99	45	51	3	-0.018	-0.019	-0.026	**0.126** *
6	1.59 - 2.25	695	280	368	47	-0.006	-0.005	-0.004	-0.027
7	2.25 - 2.31	56	21	32	3	-0.002	0.014	-0.020	0.070
8	2.31 - 3.00	537	176	319	42	-0.008	-0.005	-0.009	-0.004
9	3.00 - 3.05	32	11	20	1	-0.015	-0.012	-0.010	-0.123
10	3.05 - 3.75	395	103	285	7	-0.008	-0.003	-0.008	-0.054
11	3.75 - 3.79	19	7	12	0	0.024	**0.082** *	-0.009	-
12	3.79 - 4.50	253	110	127	16	-0.009	-0.008	-0.010	0.006
13	4.50 - 5.25	31	12	17	2	-0.006	**0.059** *	-0.044	-0.087
14	5.25 - 6.00	0	0	0	0	-	-	-	-

Table 4. Slope of linear regression of pairwise kinship coefficients on ln(distance) for each dataset. Significance was calculated by 1000 permutations of individual locations (***, $P = 0.000$; **, $P < 0.01$; *, $0.01 < P < 0.05$).

Dataset	Slope
Global	**-0.007 *** **
Between-generation	**-0.004 ***
Adults	**-0.007 ** **
Juveniles	-0.009

Kinship values at 0 m represent inbreeding coefficients (comparable to F_{IS} values) expressing the departure from Hardy-Weinberg genotypic proportions. Significance of values at 0 m was tested with 1000 permutations of gene copies among all individuals, while significance of values for distance classes was calculated by 1000 permutations of individual locations. Because analyses for each dataset were carried out at the individual level (i.e. each individual had specific spatial coordinates) and thus considering one spatial group, Loiselle's kinship coefficient at 0 m distance class was the same for global and between-generation datasets. Loiselle's kinship coefficients were highly positive and highly significant between individuals at 0 m: $F_{\text{global (between-generation)}} = 0.168$, $P = 0.000$; $F_{\text{adults}} = 0.163$, $P = 0.000$; $F_{\text{juveniles}} = 0.192$, $P = 0.000$, decreasing rapidly after that point in each dataset.

Kinship structure for the global dataset exhibited the most significant correlation and was highly similar to the kinship structure observed among adult colonies. For both datasets, after the highly positive and significant kinship values at 0 m, the mean kinship coefficient between individuals in the following distance class (0 - 0.5 m) declined substantially, but was also significantly positive and estimated to be 0.009 for global and 0.010 for adults. Thereafter, it was slowly declining and between 1.50 - 1.59 m, dropped and remained below zero, except between 3.75 - 3.79 m for global dataset, where it was positive, but not significant.

When considering juveniles, they had the highest kinship coefficient at 0 m and the steepest slope compared with other datasets, and also negative kinship value between 0 and 0.5 m, but it got significantly positive in the second (0.50 - 0.75 m) and the fifth (1.50 - 1.59 m) distance class, with values of 0.037 and 0.126, respectively. These values are in accordance with previously estimated value of the mean geographical distance (±s.d.) between half–sib colonies (0.88 ± 0.9 m).

Between-generation dataset showed similar pattern like the ones for global and adults, with kinship coefficient declining below zero between 1.50 - 1.59 m, but it had significantly positive values in 11th (3.75 - 3.79 m) and 13th (4.50 - 5.25 m) distance class, which is interesting regarding previously estimated value of the mean parent-offspring distance of 53 or 76 cm.

When considering the regression of Loiselle's kinship coefficient on geographic distance, results were similar to those previously observed with the $\hat{e}$ estimator. Global (slope = -0.007; P = 0.000) and adults (slope = −0.007; P = 0.003) datasets were characterized by a significant and similar correlation. Between-generation (slope = −0.004; P = 0.047) dataset had only marginally significant correlation, while in the juveniles (slope = -0.009; P = 0.115) dataset, it was not significant. Care must be taken in the interpretation of the juveniles analysis, because of small number of individuals, as already mentioned. From these results, it seems that adults determined most of the spatial genetic structure observed in the global dataset (Figure 10).

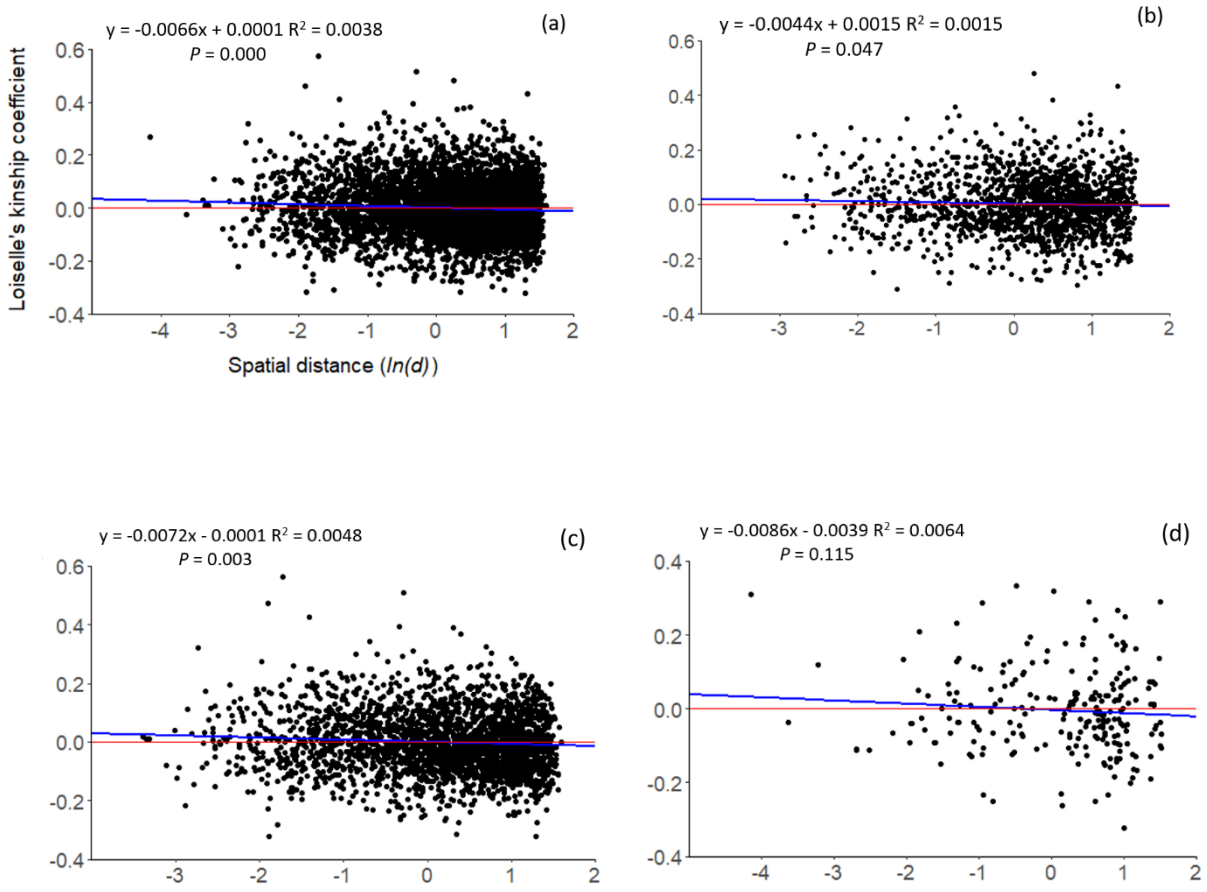

Figure 10. Loiselle's kinship coefficients plotted against logarithmic distance between (a) global, (b) adult-juvenile, (c) adults and (d) juveniles pairs of individuals. Blue line represents slope of linear regression.

Spatial autocorrelation correlograms of Loiselle's kinship coefficient within 15 distance classes for each dataset are shown in Figures 11 and 12.

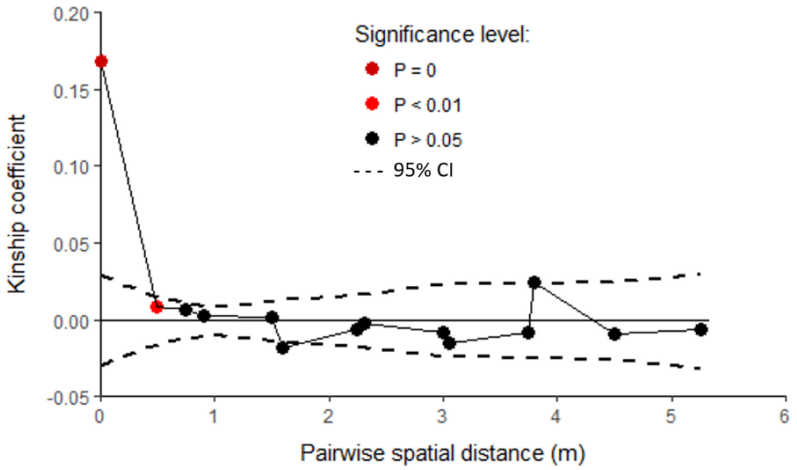

Figure 11. Average kinship coefficients, F_{ij}, between pairs of individuals plotted against the geographical distance for all red coral colonies. Dashed lines represent upper and lower limits of the 95% confidence intervals under the null hypothesis that genotypes are randomly distributed. Horizontal solid line indicates absence of spatial autocorrelation.

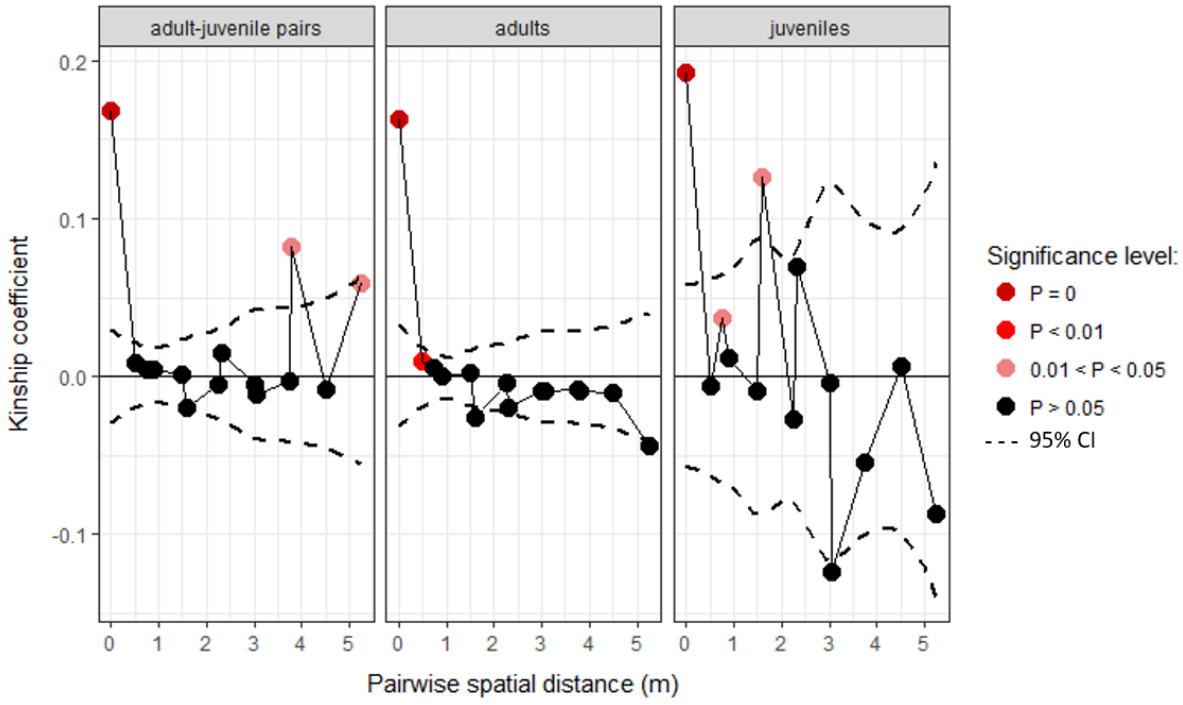

Figure 12. Average kinship coefficients, F_{ij}, between pairs of individuals plotted against the geographical distance for between-generation, adults and juveniles dataset. Dashed lines represent upper and lower limits of the 95% confidence intervals under the null hypothesis that genotypes are randomly distributed. Horizontal solid line indicates absence of spatial autocorrelation.

5.6. Inference of two demographic parameters: the 'neighbourhood size' and the gene dispersal estimates

Based on the whole data set, the neighbour size was estimated at 129 individuals (95% CI: 65 – 278 individuals), resulting in a σ_g of either 53 cm or 76 cm, assuming a census density of 36 or 18 adults/m^2, respectively (Table 5).

Table 5. Summary statistics for the linear regression analysis between geographical (*ln*(*d*)) and genetic (*ê*) distances between pairs of colonies of *Corallium rubrum* and related demographic parameters with their 95% confidence interval (***, *P* = 0.000).

Parameter	Computed value	95% CI interval
Slope	0.008 ***	0.004 - 0.015
Intercept	-0.059	-
Nb (individuals)	129	65 - 278
σ_g (cm) for De = D = 36 colonies/m^2	53	38 - 78
σ_g (cm) for De = 0.5xD = 18 colonies/m^2	76	54 - 111

6. DISCUSSION

Inferring the spatial scales at which genetic structure occurs is a crucial issue in population genetic studies on marine sessile invertebrates. Studies on genetic structuring among red coral populations were conducted at different spatial scales (from tens of meters to thousands of kilometres) and all of them revealed an extremely high level of differentiation. This result demonstrates the low connectivity of the species and, in turn, it emphasizes the importance of processes acting within population for the conservation of the species. In this context, the major goal of this study was to complement our knowledge regarding the population dynamics of the red coral by studying the pattern of spatial genetic and kinship structure within a population showing a demographic structure characteristics of protected populations (i.e. relatively low density of mid- to high sized colonies). Based on this pattern, different demographic parameters were inferred including the effective dispersal occurring during the gamete and larval phases, and the first insight in the mating pattern of this population was given.

Isolation by distance: inferences on demographic parameters

In the present study, using microsatellite markers, the occurrence of significant isolation by distance was demonstrated among colonies separated by up to 4.9 m in a population of *Corallium rubrum* harbouring the typical demographic structure of a protected population. Isolation by distance (WRIGHT, 1943) means that proximate colonies are more genetically alike than colonies further apart, due to random genetic drift and spatially restricted gene flow. When considering only the adults dataset, the relationship between genetic distance ($\hat{e}$) and the logarithm of the geographic distance remained highly significant (P = 0.000). On the contrary, IBD was not observed in juveniles. Nevertheless, whether the patterns of genetic structure varied, function of the stage-class considered requires further analyses considering the low number of juveniles and accordingly the low statistical power of the regression analyses.

According to the isolation by distance analysis using the whole dataset, the 'neighbourhood size' was estimated at 129 individuals, approximately two times larger than the value reported previously by Ledoux *et al*. (2010a). Accordingly, the estimate of the mean axial parent-offspring distance was also higher ranging between 53 and 76 cm, considering two values of D_e (36 and 18 colonies/m^2, respectively). Although 'neighbourhood size' and dispersal estimates are higher than ones reported by Ledoux *et al*. (2010a), our results confirm restricted dispersal abilities of the red coral, in the range between 10s of centimetres.

Decomposing the SGS among different stage-classes: inferences on the population dynamics of the red coral

Kinship structure analyses confirmed that neighbouring colonies are the most genetically similar. Indeed, highly positive and highly significant values of Loiselle's kinship coefficient at the 0 m for each dataset (P = 0.000) were found. In the following distance class (between 0 and 50 cm) F_{ij} values declined substantially. In the global and adults dataset, kinship coefficient kept on decreasing with increasing pairwise spatial distance, while between-generation dataset exhibited similar pattern until 3.75 m, whereupon it showed significantly positive values between 3.75 - 3.79 m and 4.50 - 5.25 m, respectively. Nevertheless, number of pairs within these two distance classes of between-generation dataset, is too low to be reliable. Juveniles showed both positive and negative kinship values without significant trend. Accounting for the stage-classes, adults were likely the main contributor to the global spatial genetic structure pattern. It is noteworthy that adults and juveniles showed different patterns of spatial genetic structure. Different hypothesis based on various demographical processes can explain these contrasting results between the two stage-classes. For instance, when the adult generation results from few founders, the strength of the FSGS is expected to be higher in adults compared to juveniles (BERENS ET AL., 2014). Nevertheless, considering the low number of juveniles analysed here, complementary works including higher number of juveniles are needed to go further in this result. A sampling focusing on different age-classes instead of stage-classes should also allow to refine this model of population dynamics.

The O-ring statistic O(*r*) showed significant spatial aggregation of individuals at small scales in the study population. Aggregation was at a scale of < 30 cm and the strongest at the 0 - 10 cm distance interval. We can assume that there is positive correlation between aggregation of red coral colonies and FSGS observed within the study population, and that genetically related individuals tend to cluster together. It is consistent with the IBD and with the highest Loiselle's kinship coefficients observed between neighbouring individuals. Our results support previous studies which have shown that the magnitude of FSGS increases with the stronger spatial aggregation of individuals (CHUNG AND CHUNG, 2013; LARA-ROMERO ET AL., 2016). To our knowledge, this is the first time that possible relationship between the spatial aggregation of individuals and FSGS has been inferred in a coral species. However, further comparative studies examining FSGS among populations with different densities and degrees of spatial aggregation are needed to better understand mechanisms generating FSGS.

Patterns of relationships and temporal genetic structure: inference on mating system.

As expected in the case of SGS, a half-sib family structure was observed. Nevertheless it seems that the network of relationships in the study population (PPL) is less dense than previously reported in the impacted populations studied by Ledoux *et al*. (2010a). Among the major differences between the two studies, the absence of parent-offspring dyads in PPL is noteworthy. This result may suggest that self-recruitment is not as important in the dynamics of PPL as it was for the impacted populations studied by Ledoux *et al*. (2010a). Demographic data demonstrated that recruitment is very low in PPL (Garrabou Pers. Obs.) explaining potentially this difference. Even if this half-sib family structure is not as marked as previously observed in this species, the occurrence of half-sib dyads confirmed that multiple mating (i.e. involvement of each parental colony in multiple mating; polygamous mating system) is likely the norm in the red coral. This result also suggested that the reproduction is done between genetically related individuals suggesting the occurrence of biparental inbreeding. Further analyses based for instance on progeny arrays are needed to confirm the occurrence of biparental inbreeding in this species. Nevertheless, it can putatively explain, in combinations with null alleles, the high positive F_{IS} value and the large deviations from panmixia leading to heterozygote deficiencies observed in this population. Such large deviations from panmixia

leading to heterozygote deficiencies have already been observed in previous studies on the red coral (ABBIATI ET AL., 1993; COSTANTINI ET AL., 2007a,b; LEDOUX ET AL., 2010b).

In long-lived species consisting of age-structured populations with overlapping generations such as the red coral, variations in the allele frequencies over a short period of time (i.e. a few generations) are expected (RYMAN, 1997). Different processes were proposed to explain this 'chaotic temporal genetic structure'. Sexually mature individuals may show differential reproductive successes leading to a random reduction of the effective population size (i.e. sweepstakes reproductive success; HEDGECOCK ET AL., 2007) and thus impacting the level of local genetic drift from one generation to the other. Alternatively, stochastic mortality during larval or the post-recruitment phases may be involved in these fluctuations. Despite this expectation, no genetic differentiation was observed between our analysed stage-classes (F_{ST} = 0) suggesting that the pool of juveniles is representative of the pool of adults. In addition, this lack of significant temporal structure suggest that the differential reproductive success among the adults is low. Once again, the low number of juveniles analyses here call for a cautious interpretation of this result. Further analyses of the genetic characterization across age-classes would help to refine our conclusion.

This study was focused on a single shallow population within marine protected area, consisting of a low density of relatively large colonies. As expected from theoretical studies (ROUSSET, 2000), the demographic characteristics observed in the study population, such as density and size structure, had an influence on the effective gene dispersal rate and the neighbourhood size. Because, the strength of local dispersal and genetic drift have major impact on determining fine-scale SGS, further comparative studies of FSGS across populations with different demographic characteristics are needed to better understand the dynamics of red coral populations.

7. CONCLUSIONS

This study refines previous findings and improves our knowledge regarding the reproductive biology and larval ecology of *C. rubrum*. By studying a protected population of red coral, the following is demonstrated:

- Significant spatial aggregation of individuals at a scale of < 30 cm
- Highly significant fine-scale spatial genetic structure with isolation by distance pattern being mainly determined by adult colonies
- The putative occurrence of density dependant processes explaining the contrasted spatial genetic structures obtained from adult and juvenile colonies
- Low values of dispersal estimates ranging between 53 and 76 cm, which are concordant with those previously reported (LEDOUX ET AL., 2010a), confirming restricted dispersal abilities and low recolonization capacities of *C. rubrum*
- A high level of half-sib family structure as a result of multiple mating
- A lack of marked differential reproductive success among adults colonies with no temporal genetic differentiation among juveniles and adults

Overall, these results highlight the importance of local processes in population biology of the red coral and accordingly in the conservation of the species.

8. REFERENCES

ABBIATI M, SANTANGELO G, NOVELLI S (1993) Genetic variation within and between two Tyrrhenian populations of the Mediterranean alcyonarian *Corallium rubrum*. Marine Ecological Progress Series 95: 245–250.

ABBIATI M, NOVELLI S, HARMELIN JC, SANTANGELO G (1997) Struttura genetica di popolamenti simpatrici e allopatici di corallo rosso. In: Cicogna F, Bavestrello G, Cattaneo-Vietti R (eds) Biologia e tutela del corallo rosso e di altri ottocoralli del Mediterraneo. Ministero delle Politiche Agricole, Rome, pp 5–21.

ARIZMENDI-MEJÍA R, LINARES C, GARRABOU J, ANTUNES A, BALLESTEROS E, CEBRIAN E, DÍAZ D, LEDOUX JB (2015) Combining genetic and demographic data for the conservation of a Mediterranean marine habitat-forming species. PloS One 10: e0119585.

AURELLE D, LEDOUX JB (2013) Interplay between isolation by distance and genetic clusters in the red coral *Corallium rubrum*: insights from simulated and empirical data. Conservation Genetics 14: 705–716.

AURELLE D, LEDOUX JB, ROCHER C, BORSA P, CHENUIL A, FÉRAL JP (2011) Phylogeography of the red coral (*Corallium rubrum*): inferences on the evolutionary history of a temperate gorgonian. Genetica 139: 855–869.

BALLESTEROS E (2006) Mediterranean coralligenous assemblages: A synthesis of present knowledge. Oceanography and marine biology 44: 123-195

BELKHIR K, BORSA P, CHIKHI L, RAUFASTE N, BONHOMME F (2004) GENETIX 4.05, logiciel sous Windows TM pour la génétique des populations. Laboratoire Génome, Populations, Interactions, CNRS UMR 5000, Université de Montpellier II, Montpellier, France.

BENJAMINI Y, HOCHBERG Y (1995) Controlling the false discovery rate – a practical and powerful approach to multiple testing. Journal of the Royal Statistical Society Series B 57: 289–300.

BERENS DG, BRAUN C, GONZÁLEZ-MARTÍNEZ SC, GRIEBELER EM, NATHAN R, BÖHNING-GAESE K (2014) Fine-scale spatial genetic dynamics over the life cycle of the tropical tree *Prunus Africana*. Heredity 113: 401–407.

BOAVIDA J, PAULO D, AURELLE D, ARNAUD-HAOND S, MARSCHAL C, REED J, GONÇALVES JM, SERRAO EA (2016) A well-kept treasure at depth: precious red coral rediscovered in Atlantic deep coral gardens (SW Portugal) after 300 years. PLoS One 11: e0147228.

BRAMANTI L, MAGAGNINI G, DE MAIO L, SANTANGELO G (2005) Recruitment, early survival and growth of the Mediterranean red coral *Corallium rubrum* (L 1758), a 4-year study. Journal of Experimental Marine Biology and Ecology 314: 69 – 78.

BRAMANTI L, VIELMINI I, ROSSI S, STOLFA S, SANTANGELO G (2011) Involvement of recreational scuba divers in emblematic species monitoring: The case of Mediterranean red coral (*Corallium rubrum*. Journal for Nature Conservation 19: 312-318.

BRAMANTI L, VIELMINI I, ROSSI S, TSOUNIS G, IANNELLI M, CATTANEO-VIETTI R, PRIORI C, SANTANGELO G (2014) Demographic parameters of two populations of red coral (*Corallium rubrum* L. 1758) in the North-Western Mediterranean. Marine Biology 161: 1015-1026.

CAU A, BRAMANTI L, CANNAS R, FOLLESA MC, ANGIOLILLO M, CANESE S, BO M, CUCCO D, GUIZIEN K (2016) Habitat constraints and self-thinning shape Mediterranean red coral deep population structure: implications for conservation practice. Scientific Reports 6: 23322.

CEBRIAN E, LINARES C, MARSCHAL C, GARRABOU J (2012) Exploring the effects of invasive algae on the persistence of gorgonian populations. Biological Invasions 14: 2647–56.

CERRANO C, BAVESTRELLO G, BIANCHI CN, CATTANEO-VIETTI R, BAVA S, MORGANTI C, MORRI C, PICCO P, SARA G, SCHIAPARELLI S, SICCARDI A, SPONGA F (2000) A catastrophic mass mortality episode of gorgonians and other organisms in the Ligurian Sea (North-western Mediterranean), summer 1999. Ecology Letters 3: 284–293.

CHAPUIS MP, ESTOUP A (2007) Microsatellite null alleles and estimation of population differentiation. Molecular Biology and Evolution 24: 621 – 631.

CHUNG MY, CHUNG MG (2013) Significant spatial aggregation and fine-scale genetic structure in the homosporous fern *Cyrtomium falcatum* (Dryopteridaceae). New Phytologist 199: 663-72.

COLL M, PIRODDI C, STEENBEEK J, KASCHNER K, BEN RAIS LASRAM F, AGUZZI J, BALLESTEROS E, BIANCHI CN, CORBERA J, DAILIANIS T, DANOVARO R, ESTRADA M, FROGLIA C, GALIL BS, GASOL JM, GERTWAGEN R, GIL J, GUILHAUMON F, KESNER-REYES K, KITSOS MS, KOUKOURAS A, LAMPADARIOU N, LAXAMANA E, LÓPEZ-FÉ DE LA CUADRA CM, LOTZE HK, MARTIN D, MOUILLOT D, ORO D, RAICEVICH S, RIUS-BARILE J, SAIZ-

SALINAS JI, SAN VICENTE C, SOMOT S, TEMPLADO J, TURON X, VAFIDIS D, VILLANUEVA R, VOULTSIADOU E (2010) The Biodiversity of the Mediterranean Sea: Estimates, Patterns, and Threats. PLoS One 5: e11842.

COSTANTINI F, ABBIATI M (2006) Development of microsatellite markers for the Mediterranean gorgonian coral *Corallium rubrum*. Molecular Ecology Notes 6: 521–523.

COSTANTINI F, FAUVELOT C, ABBIATI M (2007a) Fine-scale genetic structuring in *Corallium rubrum*: evidence of inbreeding and limited effective larval dispersal. Marine Ecology Progress Series 340: 109–119.

COSTANTINI F, FAUVELOT C, ABBIATI M (2007b) Genetic structuring of the temperate gorgonian coral (*Corallium rubrum*) across the western Mediterranean Sea revealed by microsatellites and nuclear sequences. Molecular Ecology 16: 5168–5182.

COSTANTINI F, TAVIANI M, REMIA A, PINTUS E, SCHEMBRI PJ, ABBIATI M (2010) Deep-water *Corallium rubrum* (L., 1758) from the Mediterranean Sea: Preliminary genetic characterisation. Marine Ecology 31: 261-269.

DEMPSTER AP, LAIRD NM, RUBIN DB (1977) Maximum likelihood from incomplete data via the EM algorithm. Journal of the Royal Statistical Society. Series B (Methodological) 39: 1-38.
DIFFENBAUGH N, PAL J, GIORGI F, GAO X (2007) Heat stress intensification in the Mediterranean climate change hotspot. Geophysical Research Letters 34: 1–6.

EARL DA, VON HOLDT BM (2012) STRUCTURE HARVESTER: a website and program for visualizing STRUCTURE output and implementing the Evanno method. Conservation Genetics Resources 4: 359-361.

FALUSH D, STEPHENS M, PRITCHARD JK (2003) Inference of population structure: Extensions to linked loci and correlated allele frequencies. Genetics 164: 1567–1587.

FRANKHAM R (2005). Genetics and extinction. Biolological Conservation 126: 131–140.

GARRABOU J, COMA R, BENSOUSSAN N, BALLY M, CHEVALDONNÉ P, CIGLIANO M, DIAZ D, HARMELIN JG, GAMBI CM, KERSTING DK, LEDOUX JB, LEJEUSNE C, LINARES C, MARSCHAL C, PEREZ T, RIBES M, ROMANO C, SERRANO E, TEIXIDO N, TORRENTS O, ZABALA M, ZUBERER F, CERRANO C (2009) Mass mortality in

Northwestern Mediterranean rocky benthic communities: effects of the 2003 heat wave. Global Change Biology 15: 1090–1103.

GARRABOU J, HARMELIN JG (2002) A 20-year study on life-history traits of a harvested long-lived temperate coral in the NW Mediterranean: Insights into conservation and management needs. Journal of Animal Ecology 71: 966-978.

GARRABOU J, PEREZ T, SARTORETTO S (2001) Mass mortality event in red coral *Corallium rubrum* populations in the Provence region (France, NW Mediterranean). Marine Ecology Progress Series 217: 263–272.

GARRABOU J, SALA E, LINARES C, LEDOUX JB, MONTERO-SERRA I, DOMINICI JM, KIPSON S, TEIXIDÓ N, CEBRIAN E, KERSTING DK, HARMELIN JG (2017) Re-shifting the ecological baseline for the overexploited Mediterranean red coral. Scientific Reports 7: 42404.

Gili JM, Coma R (1988) Benthic suspension feeders: their paramount role in littoral marine food webs. Trends in Ecology & Evolution 13: 316–1.

GOUDET J (1995) FSTAT (vers. 1.2): a computer program to calculate F-statistics. J. Heredity 86: 485-486.

GRAHAM NA, NASH KL (2013) The importance of structural complexity in coral reef ecosystems. Coral Reefs 32: 315–26.

GRUSSENMEYER P, DRAP P (2000) ARPENTEUR: a web-based photogrammetry tool for architectural modelling. Proc. SPIE 4309, Videometrics and Optical Methods for 3D Shape Measurement

GUO S, THOMPSON E (1992) Performing the exact test of Hardy–Weinberg proportion for multiple alleles. Biometrics 48: 361–372.

HALPERN BS, WALBRIDGE S, SELKOE KA, KAPPEL CV, MICHELI F, D'AGROSA C, BRUNO JF, CASEY KS, EBERT C, FOX HE, FUJITA R, HEINEMANN D, LENIHAN HS, MADIN EM, PERRY MT, SELIG ER, SPALDING M, STENECK R, WATSON R (2008) A Global Map of Human Impact on Marine Ecosystems. Science 319: 948–952.

HARDY OJ, VEKEMANS X (2002) SPAGeDi: a versatile computer program to analyse spatial genetic structure at the individual or population levels. Molecular Ecology Notes 2: 618-620.

HARE MP, NUNNEY L, SCHWARTZ MK, RUZZANTE DE, BURFORD M, WAPLES RD, RUEGG K, PALSTRA F (2011) Understanding and estimating effective population size for practical application in marine species management. Conservation Biology 25: 438–449.

HARLEY CDG, HUGHES AR, HULTGREN KM, MINER BG, SORTE CJ, THORNBER CS, RODRIGUEZ LF, TOMANEK L, WILLIAMS SL (2006) The impacts of climate change in coastal marine systems. Ecology Letters 9: 228–241.

HARPER JL, WHITE J (1974) The Demography of Plants. Annual Review of Ecology and Systematics 5: 419-463.

HARTL DL AND CLARK AG (1989) Principles of Population Genetics 2nd edition Sinauer Associates Inc, Sunderland MA.

HEDGECOCK D, LAUNEY S, PUDOVKIN AI, NACIRI Y, LAPÈGUE S, BONHOMME F (2007) Small effective number of parents (Nb) inferred for a naturally spawned cohort of juvenile European flat oysters *Ostrea edulis*. Marine Biology 150: 1173–1182.

HENDRY AP, LOHMANN LG, CONTI E, CRACRAFT J, CRANDALL KA, FAITH DP, HÄUSER C, JOLY CA, KOGURE K, LARIGAUDERIE A, MAGALLÓN S, MORITZ C, TILLIER S, ZARDOYA R, PRIEUR-RICHARD AH, WALTHER BA, YAHARA T, DONOGHUE MJ (2010) Evolutionary biology in biodiversity science, conservation, and policy: a call to action. Evolution 64: 1517-28.

HUGHES TP (1994) Catastrophes, phase shifts and large scale degradation of a Caribbean coral reef. Science 265: 1547–9.

IPCC (2007) Climate change 2007: the physical science basis. Contribution of working group I to the Fourth Assesment. Report of the intergovernmental panel on climate change (eds SOLOMON SD, QIN M, MANNING Z, et al.), 996 pp. Cambridge University Press, Cambridge, UK and New York, NY, USA.

JONES OR, WANG J (2010) COLONY: A program for parentage and sibship inference from multilocus genotype data. Molecular Ecology Resources 10: 551-5.

KENDALL M, STEWART A (1977). The advanced Theory of statistics, volume 1. Macmillan, New York.

KIPSON S, FOURT M, TEIXIDÓ N, CEBRIAN E, CASAS E, BALLESTEROS E, ZABALA M, GARRABOU J (2011) Rapid biodiversity assessment and monitoring method for highly diverse benthic communities: a case study of mediterranean coralligenous outcrops. PLoS One 6: e27103.

KNITTWEIS L, AGUILAR R, ALVAREZ H, BORG JA, EVANS J, GARCIA S, SCHEMBRI PJ (2016) New Depth Record of the Precious Red Coral *Corallium rubrum* for the Mediterranean. Rapport du Congrès de la Commission Internationale pour l'Exploration Scientifique de la Mer Méditerranée 41: 467.

LARA-ROMERO C, GARCÍA-FERNÁNDEZ A, ROBLEDO-ARNUNCIO JJ, ROUMET M, MORENTE-LÓPEZ J, LÓPEZ-GIL A, IRIONDO JM (2016) Individual spatial aggregation correlates with between-population variation in fine-scale genetic structure of *Silene ciliata* (Caryophyllaceae). Heredity 116: 417-23.

LEDOUX JB, GARRABOU J, BIANCHIMANI O, DRAP P, FÉRAL JP, AURELLE D (2010a) Fine-scale genetic structure and inferences on population biology in the threatened Mediterranean red coral, *Corallium rubrum*. Molecular Ecology 19: 4204–16.

LEDOUX J B, MOKTHAR-JAMAI K, ROBY C, FÉRAL J P, GARRABOU J (2010b) Genetic survey of shallow populations of the Mediterranean red coral [*Corallium rubrum* (Linnaeus, 1758)]: new insights into evolutionary processes shaping nuclear diversity and implications for conservation. Molecular Ecology 19: 675-690.

LINARES C, BIANCHIMANI O, TORRENTS O MARSCHAL C, DRAP P, GARRABOU J (2010) Marine Protected Areas and the conservation of long-lived marine invertebrates: the Mediterranean red coral. Marine Ecology Progress Series 402: 69–79.

LOISELLE BA, SORK VL, NASON J, GRAHAM C (1995) Spatial genetic structure of a tropical understory shrub, *Psychotria officinalis* (Rubiaceae). American Journal of Botany 82: 1420–1425.

LOWE WH, ALLENDORF FW (2010) What can genetics tell us about population connectivity? Molecular Ecology 19: 3038–3051.

MARSCHAL C, GARRABOU J, HARMELIN JG., PICHON M (2004) A new method for measuring growth and age in the precious red coral *Corallium rubrum* (L.). Coral Reefs 23: 423-432.

MILLER SA, DYKES DD, POLESKY HF (1988) A simple salting out procedure for extracting DNA from human nucleated cells. Nucleic Acids Research 16: 1215.

NEI M (1973) Analysis of gene diversity in subdivided populations. Proceedings of the National Academy of Sciences of the United States of America 70: 3321–3323.

PALUMBI SR (2003) Population genetics, demographic connectivity, and the design of marine reserves. Ecological Applications 13: S146–S158.

PETIT RJ, MOUSADIK AE, PONS O (1998) Identifying populations for conservation on the basis of genetic markers. Conservation Biology 12: 844–855.

PINSKY ML, PALUMBI SR (2014) Meta-analysis reveals lower genetic diversity in overfished populations. Molecular Ecology 23: 29–39.

PONTI M, PERLINI RA, VENTRA V, GRECH D, ABBIATI M, CERRANO C (2014) Ecological shifts in Mediterranean coralligenous assemblages related to gorgonian forest loss. PLoS One. 9: e102782.

PRIORI C, MASTASCUSA V, ERRA F, ANGIOLILLO M, CANESE S, SANTANGELO G (2013) Demography of deep-dwelling red coral populations: Age and reproductive structure of a highly valued marine species. Estuarine Coastal and Shelf Science 118: 43-49.

PRITCHARD JK, STEPHENS M, DONNELLY P (2000) Inference of population structure using multilocus genotype data. Genetics 155: 945–959.

ROSSI S (2013) The destruction of the 'animal forests' in the oceans: towards an over-simplification of the benthic ecosystems. Ocean & Coastal Management 84: 77–85.

ROSSI S, TSOUNIS G, OREJAS C, PADRÓN T, GILI JM, BRAMANTI L, TEIXIDÓ N, GUTT J (2008) Survey of deep-dwelling red coral (*Corallium rubrum*) populations at Cap de Creus (NW Mediterranean). Marine Biology 154: 533–545.

ROUSSET F (2000) Genetic differentiation between individuals. Journal of Evolutionary Biology 13: 58–62.

ROUSSET F (2008) GENEPOP'007: a complete re-implementation of the GENEPOP software for Windows and Linux. Molecular Ecology Resources 8: 103–106.

ROYER JP, NAWAF MM, MERAD D, SACCONE M, BIANCHIMANI O, GARRABOU J, LEDOUX JB, LOPEZ-SANZ A, DRAP P (2018) Photogrammetric Surveys and Geometric Processes to Analyse and Monitor Red Coral Colonies. Journal of Marine Science and Engineering 6, 42.

RYMAN N (1997) Minimizing adverse effects of fish culture: understanding the genetics of populations with overlapping generations. ICES Journal of Marine Science 54: 1149–1159.

SANTANGELO G, CARLETTI E, MAGGI E, BRAMANTI L (2003) Reproduction and population sexual structure of the overexploited Mediterranean red coral *Corallium rubrum*. Marine Ecology Progress Series 248: 99-108.

SERRANO XM, BAUMS IB, SMITH TB, JONES RJ, SHEARER TL, BAKER AC (2016) Long distance dispersal and vertical gene flow in the Caribbean brooding coral *Porites astreoides*. Scientific Reports 6: 21619.

STOCKWELL CA, HENDRY AP, KINNISON MT (2003) Contemporary evolution meets conservation biology. Trends in Ecology & Evolution 18: 94–101.

TAVIANI M, FREIWALD A, BEUCK L, ANGELETTI L, REMIA A (2010) The deepest known occurrence of the precious red coral *Corallium rubrum* (L. 1758) in the Mediterranean Sea. In: Bussoletti E., Cottingham D., Bruckner A., Roberts G., Sandulli R. (Eds), Proceedings of the International Workshop on Red Coral Science, Management, Trade: Lessons from the Mediterranean. NOOA Technical Memorandum, Silver Spring, MA, CRCP-13, 87–93.

TEMPLETON AR (2006) Population Genetics and Microevolutionary Theory. John Wiley & Sons, Hoboken, New Jersey.

TOONEN RJ, HUGHES S (2001) Increased Throughput for Fragment Analysis on ABI Prism 377 Automated Sequencer Using a Membrane Comb and STRand Software. Biotechniques 31: 1320-1324.

TORRENTS O, GARRABOU J, MARSCHAL C, HARMELIN JG (2005) Age and size at first reproduction in the commercially exploited red coral *Corallium rubrum* (L.) in the Marseilles area (France, NW Mediterranean). Biological Conservation 121: 391–397.

TSOUNIS G, ROSSI S, BRAMANTI L, SANTANGELO G (2013) Management hurdles for sustainable harvesting of *Corallium rubrum*. Marine Policy 39: 361–364.

TSOUNIS G, ROSSI S, GILI J M, ARNTZ W (2006) Population structure of an exploited benthic cnidarian: The case study of red coral (*Corallium rubrum* L.). Marine Biology 149: 1059-1070.

UNDERWOOD JN, SMITH LD, VAN OPPEN MJH, GILMOUR JP (2009) Ecologically relevant dispersal of corals on isolated reefs: implications for managing resilience. Ecological Applications 19: 18–29.

VALIÈRE N (2002) GIMLET: a computer program for analysing genetic individual identification data. Molecular Ecology Notes 2: 377–379.

VAN OOSTERHOUT C, HUTCHINSON WF, WILLS DPM, SHIPLEY P (2004) MICRO-CHECKER: software for identifying and correcting genotyping errors in microsatellite data. Molecular Ecology Notes 4: 535–538.

VEKEMANS X, HARDY OJ (2004) New insights from fine-scale spatial genetic structure analyses in plant populations. Molecular Ecology 13: 921–935.

VIGHI M (1972) Etude sur la reproduction du *Corallium rubrum* (L.). Vie et Milieu 23: 21–32.

WALTHER G-R, POST E, CONVEY P, MENZEL A, PARMESAN C, BEEBEE TJ, FROMENTIN JM, HOEGH-GULDBERG O, BAIRLEIN F (2002) Ecological responses to recent climate change. Nature 416: 389–395.

WANG J, SANTURE A (2009) Parentage and sibship inference from multilocus genotype data under polygamy. Genetics 181: 1579–1594.

WATTS PC, ROUSSET F, SACCHERI IJ, LEBLOIS R, KEMP SJ, THOMPSON DJ (2007) Compatible genetic and ecological estimates of dispersal rates in insect (*Coenagrion mercurial*: Odonata: Zygoptera) populations: analysis of 'neighbourhood size' using a more precise estimator. Molecular Ecology 16: 737–751.

WEINBERG S (1979) The light-dependent behaviour of planula larvae of *Eunicella singularis* and *Corallium rubrum* and its implication for octocorallian ecology. Bijdragen tot de Dierkunde, 49: 16–30.

WEIR BS, COCKERHAM CC (1984) Estimating F-statistics for the analysis of population structure. Evolution 38: 1358–1370.

WIEGAND T, MOLONEY KA (2004) Rings, circles, and null-models for point pattern analysis in ecology. Oikos 104: 209–229.

WIEGAND T, MOLONEY KA (2014) A handbook of spatial point pattern analysis in ecology. Chapman and Hall/CRC press, Boca Raton, FL.

WRIGHT S (1943) Isolation by distance. Genetics 28: 114–138.

9. APPENDICES

Appendix 1

DNA extraction protocol: salting out procedure, adjusted from Miller *et al*. (1988).

Appendix 2

Height and diameter measurements, as well as spatial position (x,y) of *Corallium rubrum* colonies within the study plot (Passe Palazzu, Corsica, France).

Appendix 3

Microsatellite genotypes of *Corallium rubrum* colonies used for genetic analyses.

Appendix 1

DNA extraction protocol: salting out procedure, adjusted from Miller *et al*. (1988).

1. For each colony/individual dissect around 10 polyps in a Petri dish with a clean scalpel
2. Incubation few minutes at 55°C to dry the remaining alcohol
3. Add 300 µL of TNES buffer
4. Add 10 µL of proteinase K (20 mg/mL) + vortex + centrifuge
5. Incubation at 55°C for 4 to 5 hours
6. Put the digestion product in a new tube (without any remaining tissue)
7. Add 84 µL of NaCl (6M) (during this step the proteins will be precipitated)
8. Centrifugation for 15 min at 10000 g or 10,0 rcf or 12,2 rpm
9. Put the supernatant in a new tube
10. Add 390 µL of cold (-20°C) absolute alcohol (ethanol 100%)
11. Add 39 µL of Sodium Acetate (3M, pH=7)
12. Centrifugation for 15 min at 13000 g or 13,0 rcf or 13,9 rpm (DNA precipitation)
13. Remove the alcohol by pipetting
14. Add 390 µL of cold 70% ethanol
15. Centrifugation for 15 min at 13000 g
16. Remove the alcohol
17. Let the tubes dry over night
18. If needed, incubation for few minutes at 55°C to remove the remaining alcohol
19. Add 50-100 µL of Milli-Q sterilized H_2O

Appendix 2

Height and diameter measurements, as well as spatial position (x,y) of *Corallium rubrum* colonies within the study plot (Passe Palazzu, Corsica, France). Individuals marked in blue were assigned to juveniles.

			Spatial position (m)	
IND	Height (mm)	Diameter (mm)	x	y
PPL1	54.44123764	10.0266867	-2.17	-0.751
PPL2	28.702	4.236617914	-1.994	-0.798
PPL3	43.50436753	0	-1.797	-0.782
PPL4	26.688	0	-2.048	-0.666
PPL5	49.28996621	10.99048418	-1.986	-0.693
PPL6	21.29675022	0	-1.928	-0.71
PPL7	47.78039796	0	-2.013	-0.575
PPL8	38.39308455	0	-1.863	-0.648
PPL9	39.72240659	5.69344485	-1.813	-0.669
PPL10	44.26457115	6.546944997	-1.702	-0.667
PPL11	25.6000244	3.163	-1.715	-0.626
PPL14	20.92605278	0	-1.615	-0.731
PPL15	25.18980164	0	-1.568	-0.69
PPL16	35.79224063	5.989918103	-1.604	-0.638
PPL17	46.85692382	0	-1.557	-0.62
PPL18	43.34629253	0	-1.596	-0.562
PPL19	32.76444623	0	-1.501	-0.707
PPL20	72.50284177	17.70372202	-1.472	-0.608
PPL21	28.178	3.388	-1.4	-0.594
PPL22	28.954	3.894	-1.384	-0.592
PPL23	29.379	0	-1.458	-0.56
PPL24	36.821	8.406	-1.349	-0.657
PPL25	42.01111371	9.431	-1.328	-0.759
PPL26	63.606	14.807	-1.264	-0.62
PPL27	57.218	0	-1.182	-0.65
PPL28	-	-	-1.095	-0.711
PPL29	56.085	0	-1.157	-0.482
PPL30	40.689	7.533	-1.118	-0.513
PPL31	34.01199316	0	-1.152	-0.638
PPL34	77.51540793	8.876	-1.023	-0.582
PPL35	82.459	0	-0.981	-0.461
PPL36	55.78454417	0	-0.916	-0.514
PPL37	-	-	-0.869	-0.688
PPL38	-	-	-0.805	-0.662

			Spatial position (m)	
IND	Height (mm)	Diameter (mm)	x	y
PPL39	56.01031974	0	-0.96	-0.382
PPL40	55.521	8.069	-0.875	-0.445
PPL41	77.734	0	-0.789	-0.367
PPL42	54.497	0	-0.797	-0.448
PPL43	85.252	0	-0.728	-0.485
PPL44	46.287	0	-0.704	-0.43
PPL45	41.679	7.772	-0.655	-0.493
PPL46	46.00183995	0	-0.661	-0.439
PPL47	73.90865222	0	-0.626	-0.433
PPL48	64.21052262	0	-0.586	-0.373
PPL49	-	-	-0.394	-0.537
PPL50	44.534	0	-0.365	-0.371
PPL51	41.243	0	-0.39	-0.347
PPL52	93.947	0	-0.28	-0.264
PPL53	5.3893978	3.415289332	-0.265	-0.423
PPL54	23.841	4.094	-0.202	-0.159
PPL55	47.752	0	-0.188	-0.168
PPL57			-0.12	-0.361
PPL58	48.833	7.06	0.013	-0.305
PPL59	29.594	4.83	-0.059	-0.297
PPL60	74.481	0	-0.015	-0.164
PPL61	75.886	0	0.057	-0.299
PPL62	75.98891191	0	0.12	-0.282
PPL64	55.62296657	0	0.228	-0.143
PPL65	21.86417167	3.087168105	0.132	-0.111
PPL66	37.49236508	4.452117719	0.231	-0.085
PPL67	12.949	0	0.357	-0.193
PPL68	10.15207634	5.496989354	0.388	-0.214
PPL69	65.457	0	0.54	-0.128
PPL70	28.11965364	0	0.549	-0.006
PPL71	57.8307297	0	0.67	-0.163
PPL72	82.504	0	0.658	-0.074
PPL73	21.53355469	0	0.714	-0.051
PPL74	35.977	0	0.746	-0.17
PPL75	99.75461559	0	0.871	-0.151
PPL76	86.599	0	0.922	-0.099
PPL77	16.9802868	0	0.931	-0.025
PPL78	44.42878984	0	0.993	-0.064
PPL79	79.15720118	0	1.045	-0.103
PPL80	55.78960307	0	1.057	-0.059
PPL81	25.398	4.478	1.062	0.026
PPL82	30.72349367	0	1.088	0.025
PPL83	82.981	0	1.219	-0.098

			Spatial position (m)	
IND	Height (mm)	Diameter (mm)	x	y
PPL84			1.292	-0.278
PPL85	67.177	0	1.348	-0.131
PPL86	89.596	0	1.786	-0.184
PPL87	80.005	0	1.77	-0.089
PPL88	93.878	0	1.888	-0.025
PPL89	74.617	15.621	2.023	-0.071
PPL90	46.71050389	0	2.054	0.026
PPL91	78.834	17.443	2.104	-0.061
PPL92	-	-	2.13	-0.153
PPL93	69.098	0	2.163	-0.032
PPL94	35.403	0	2.244	0.036
PPL95	65.276	7.304	2.311	-0.023
PPL96	78.22252181	0	2.324	-0.151
PPL97	45.74260601	7.032571271	2.383	-0.101
PPL98	15.66454171	0	2.462	-0.019
PPL99	35.714	0	2.36	0.055
PPL100	56.398	0	2.469	0.039
PPL101	30.43183622	0	2.367	0.108
PPL104	94.22620116	0	2.67	-0.08
PPL106	54.769	0	2.522	0.136

Appendix 3

Microsatellite genotypes of *Corallium rubrum* colonies used for genetic analyses.

IND	Mic13		Mic20		Mic22		Mic23		Mic24		Mic25		Mic26		Mic27		COR46	
PPL1	133	137	200	200	168	174	095	103	147	229	000	000	158	188	451	459	175	207
PPL2	133	133	200	200	168	172	105	105	183	227	147	147	160	182	000	000	000	000
PPL3	137	137	200	200	168	168	103	105	147	183	147	147	166	186	000	000	000	000
PPL4	133	133	200	200	168	168	103	103	207	219	159	159	158	182	000	000	213	213
PPL5	133	135	200	200	172	172	095	105	219	221	131	187	176	182	181	181	000	000
PPL6	133	133	200	282	168	168	095	101	177	181	155	159	160	164	181	181	000	000
PPL7	137	137	200	200	168	172	095	103	175	179	161	161	158	188	183	183	000	000
PPL8	133	133	200	200	172	182	095	095	151	203	139	139	158	160	181	181	000	000
PPL9	133	133	200	200	172	172	103	105	147	181	000	000	156	192	181	181	000	000
PPL10	135	135	204	204	000	000	000	000	000	000	000	000	160	160	000	000	000	000
PPL11	133	137	200	200	168	172	095	101	207	229	155	155	166	188	173	173	000	000
PPL14	137	137	284	284	172	172	121	123	173	177	131	131	158	180	177	181	000	000
PPL15	133	133	200	200	168	172	115	125	181	233	155	155	158	188	000	000	000	000
PPL16	133	133	200	262	168	168	095	103	147	207	155	155	158	188	183	183	201	201
PPL17	133	137	200	200	172	172	103	107	221	225	147	155	172	184	193	193	213	215
PPL18	131	137	200	200	172	172	103	107	147	219	131	147	158	160	197	197	195	213
PPL19	133	133	200	200	000	000	095	097	173	173	000	000	176	186	377	385	195	209
PPL20	133	133	200	262	168	170	105	123	147	147	147	159	160	180	181	181	201	213
PPL21	131	133	206	284	168	168	095	095	173	183	131	147	158	166	000	000	195	195
PPL22	133	137	202	262	168	168	095	103	207	225	147	147	166	166	000	000	175	201
PPL23	133	133	200	200	168	172	105	121	201	207	159	159	158	182	181	447	000	000
PPL24	133	133	262	262	168	168	105	105	177	185	147	159	158	160	173	177	000	000
PPL25	131	133	200	200	172	172	101	101	207	207	131	159	158	160	183	183	175	213
PPL26	133	133	200	262	168	168	103	103	183	185	139	139	166	166	171	185	195	209
PPL27	133	133	200	200	172	172	103	103	169	219	000	000	182	184	000	000	209	211
PPL28	133	133	200	200	172	172	101	105	207	207	131	131	158	180	000	000	207	209
PPL29	133	135	200	262	162	168	101	103	201	225	147	147	158	184	000	000	175	175
PPL30	137	137	200	200	168	168	095	095	147	177	155	155	180	180	181	197	000	000
PPL31	135	135	200	200	168	172	103	123	173	229	147	155	160	166	185	185	175	209

IND	Mic13		Mic20		Mic22		Mic23		Mic24		Mic25		Mic26		Mic27		COR46	
PPL34	133	133	200	200	172	172	103	105	181	207	131	131	158	180	377	389	209	213
PPL35	133	135	200	262	162	168	101	103	201	225	147	147	158	184	405	405	175	201
PPL36	133	133	200	200	168	168	095	103	147	177	155	155	166	184	451	451	175	209
PPL37	133	133	200	262	172	174	095	105	177	183	147	155	182	184	435	435	195	195
PPL38	133	133	200	200	172	182	095	101	173	219	147	147	184	186	181	181	207	207
PPL39	133	133	200	262	172	172	095	103	219	225	155	159	178	186	183	183	195	195
PPL40	133	133	200	202	168	172	101	103	177	219	155	159	166	182	187	189	175	195
PPL41	133	133	200	200	168	172	103	105	177	219	147	147	160	160	191	191	195	209
PPL42	133	133	200	262	168	172	095	103	177	207	147	155	158	180	173	183	195	201
PPL43	133	137	200	262	172	182	101	105	219	227	159	159	180	186	389	389	195	207
PPL44	133	133	200	200	168	168	095	121	219	221	147	147	184	184	000	000	175	201
PPL45	133	133	202	262	168	168	101	103	181	185	135	165	158	174	000	000	195	207
PPL46	135	135	200	200	172	172	095	101	173	177	000	000	176	184	181	181	195	209
PPL47	133	137	200	202	168	172	095	103	177	219	155	155	164	182	000	000	215	219
PPL48	131	133	200	262	172	172	095	105	147	147	147	159	160	184	000	000	177	195
PPL49	133	133	200	200	168	172	095	105	173	177	147	147	164	166	191	451	201	215
PPL50	131	133	200	200	168	172	101	103	227	229	131	147	180	184	000	000	175	195
PPL51	137	137	200	200	168	168	103	107	183	201	155	155	164	180	179	385	195	213
PPL52	131	131	200	202	168	172	103	107	169	219	147	159	160	186	173	183	177	215
PPL53	133	133	200	200	172	172	101	103	181	231	159	159	164	182	381	405	195	213
PPL54	131	133	200	200	168	172	105	123	173	177	131	159	160	180	181	181	175	195
PPL55	131	133	200	200	168	172	105	123	173	177	131	159	160	180	181	181	175	195
PPL57	133	135	200	200	172	172	095	101	147	169	155	155	180	184	177	181	195	207
PPL58	133	137	200	200	168	168	105	107	181	201	159	159	166	166	185	185	195	195
PPL59	133	135	200	200	168	172	095	103	169	207	147	155	164	180	177	177	195	195
PPL60	133	133	200	202	168	168	103	105	173	221	131	155	160	166	183	183	175	209
PPL61	133	133	200	200	168	172	103	105	177	183	131	155	182	184	000	000	195	195
PPL62	133	133	200	200	168	172	103	105	177	183	131	155	182	184	000	000	000	000
PPL64	133	137	200	262	168	168	103	107	221	221	147	147	164	178	175	175	195	195
PPL65	133	133	200	200	172	172	103	107	183	233	147	147	180	182	173	179	195	207
PPL66	133	133	200	200	168	172	095	101	147	183	147	147	160	166	000	000	195	215
PPL67	133	133	200	200	168	172	095	105	177	181	147	147	158	178	000	000	195	209
PPL68	133	133	200	200	168	172	101	105	225	227	147	147	174	180	389	393	175	195
PPL69	133	133	200	200	172	182	103	103	221	231	159	159	158	164	181	181	177	207

IND	Mic13		Mic20		Mic22		Mic23		Mic24		Mic25		Mic26		Mic27		COR46	
PPL70	135	135	200	200	172	172	095	105	177	221	147	147	160	172	181	181	195	195
PPL71	133	133	200	200	168	172	095	105	183	225	131	147	180	182	451	451	175	195
PPL72	137	137	200	200	172	172	103	103	177	181	155	159	158	174	181	451	195	195
PPL73	133	133	200	200	168	172	101	103	147	173	131	131	166	184	181	181	195	213
PPL74	133	133	200	202	172	172	095	103	147	221	131	131	158	178	000	000	215	215
PPL75	133	135	200	202	168	172	103	103	173	227	147	155	160	174	181	181	207	215
PPL76	133	133	200	200	172	172	101	103	173	233	000	000	158	180	181	181	209	213
PPL77	135	135	200	200	172	172	095	103	183	221	131	155	176	184	177	177	195	195
PPL78	133	135	200	200	172	172	103	105	147	221	147	155	160	166	181	181	201	201
PPL79	133	133	200	200	168	168	103	107	177	181	155	155	158	166	181	181	195	215
PPL80	133	133	200	200	168	168	103	107	177	181	155	155	158	166	181	181	195	215
PPL81	133	133	200	200	172	172	101	105	177	207	147	147	158	166	451	455	000	000
PPL82	133	133	200	206	172	174	105	107	181	181	155	155	160	180	175	175	175	195
PPL83	133	133	200	200	168	172	095	103	183	219	147	147	166	166	179	179	000	000
PPL84	133	135	200	200	168	172	095	105	221	221	147	147	156	184	165	177	000	000
PPL85	133	133	200	200	168	172	103	105	173	219	131	147	166	166	181	181	195	195
PPL86	133	133	200	200	168	172	095	101	173	179	131	131	160	160	000	000	000	000
PPL87	133	133	200	200	172	172	095	105	181	185	131	155	166	166	000	000	195	221
PPL88	133	133	200	200	168	168	107	123	169	173	131	131	166	184	000	000	205	213
PPL89	133	133	200	200	168	168	101	105	181	225	000	000	156	166	181	181	000	000
PPL90	133	137	200	200	172	172	123	123	177	225	131	131	158	166	185	185	195	195
PPL91	133	133	200	284	168	172	101	123	227	229	167	167	158	166	000	000	000	000
PPL92	133	133	200	200	168	168	101	103	147	201	131	147	156	158	173	193	195	207
PPL93	133	133	200	200	168	172	103	105	173	221	147	147	180	186	181	181	000	000
PPL94	133	133	200	200	168	172	101	107	173	201	131	147	156	158	197	197	201	201
PPL95	133	133	200	200	168	172	103	107	169	173	131	131	180	184	000	000	195	209
PPL96	133	137	200	284	168	172	095	101	169	225	155	167	160	186	000	000	195	201
PPL97	133	133	200	200	168	168	095	105	181	233	147	167	160	180	157	181	195	213
PPL98	133	133	200	200	172	172	095	103	177	181	131	173	164	186	177	183	000	000
PPL99	133	133	200	200	172	172	101	105	169	233	147	155	160	184	181	451	175	195
PPL100	133	133	200	200	172	172	103	107	181	219	147	147	166	182	000	000	195	195
PPL101	133	133	200	200	168	168	101	103	173	181	131	131	156	158	181	183	201	213
PPL104	133	133	200	200	168	168	101	103	169	173	000	000	166	182	181	197	175	195
PPL106	133	133	200	200	168	174	095	101	183	225	147	167	174	182	177	177	195	213

10. BIOGRAPHY

Personal information

- Date and place of birth: 02/06/1988, Split, Croatia
- Residence address: Vukovarska 7, Kaštel Stari, 21216
- Mobile phone: +385 977182417
- E-mail: sstipoljev@yahoo.com

Education

- Erasmus+ traineeship (6 months)
  Institut de Ciències del Mar - Consejo superior de Investigaciones Científicas (CSIC), Barcelona, Spain
- Bachelor Degree in Molecular Biology
  Faculty of Science, Zagreb, Croatia
- High school graduate
  Opća gimnazija "Braća Radić", Kaštel Štafilić, Croatia

Training

- Laboratory skill training (6 months) within project 'Molekularna epidemiologija nekih invazijskih oboljenja divljih životinja' (Molecular epidemiology of some invasive wildlife diseases) leaded by Dean Konjević
  Faculty of Science, Department of Biology, Division of Animal Physiology, Zagreb, Croatia

Congress and conference papers

- Arbanasić H, Galov A, Vranković L, **Stipoljev S**, Šprem N, Bujanić M, Konjević D (2016) Variability of major histocompatibility complex class II DRB1 locus in wild boar (Sus scrofa L.) from Croatia – preliminary observations. 3rd International Vetistanbul Group Congress 2016, Sarajevo, Bosnia and Herzegovina, May 17-20, 2016
- Arbanasić H, Galov A, Vranković L, **Stipoljev S**, Šprem N, Bujanić M, Konjević D (2017) Comparison of the PCR methods for assessing variability of major histocompatibility complex class II DRB1 locus in wild boar (Sus scrofa L.) from Croatia. Proceedings of the 3rd International conference on avian herpetological and exotic mammal medicine. March 25th – 29th 2017, Venice, Italy

Research Paper

In revision:

- Arbanasić H, Konjević D, Vranković L, Bujanić M, **Stipoljev S**, Balažin M, Šprem N, Galov A Evolution of MHC class II DRB1 locus in the Croatian wild boar (*Sus scrofa*) implies duplication and weak signals of positive selection.